Article

The DUX4-HIF1α Axis in Murine and Human Muscle Cells: A Link More Complex than Expected

Thuy-Hang Nguyen[1], Sihame Bouhmidi[1], Lise Paprzycki[1], Alexandre Legrand[1], Anne-Emilie Declèves[2], Philipp Heher[3], Alexandra Belayew[1], Christopher R. S. Banerji[3], Peter S. Zammit[3], Alexandra Tassin[*]

[1] Laboratory of Respiratory Physiology, Pathophysiology and Rehabilitation, Research Institute for Health Sciences and Technology, University of Mons, Mons, 7000, Belgium; thuyhang.nguyen@umons.ac.be (T.-H.N.); lise.paprzycki@student.umons.ac.be (L.P.); Bouhmidi-sihame@hotmail.com (S.B.); alexandra.belayew@umons.ac.be (A.B.); alexandre.legrand@umons.ac.be (A.L.)

[2] Department of Metabolic and Molecular Biochemistry, Research Institute for Health Sciences and Technology, University of Mons, Mons, 7000, Belgium; anne-emilie.decleves@umons.ac.be (A-E.D.)

[3] Randall Centre for Cell and Molecular Biophysics, King's College London, Guy's Campus, London, UK; philipp.heher@kcl.ac.uk (P.H.); christopher.banerji@gstt.nhs.uk (CRS.B.); peter.zammit@kcl.ac.uk (PS.Z.)

[*] Correspondence: alexandra.tassin@umons.ac.be (A.T.)

Abstract: FacioScapuloHumeral Dystrophy (FSHD) is one of the most frequent inherited muscle disorders, and is linked to the inappropriate expression of the DUX4 transcription factor in adult muscles. The deregulated molecular network causing FSHD skeletal muscle dysfunction and pathology is still not well understood. It has been shown that the hypoxia response factor HIF1α is critically disturbed in FSHD and has a major role in DUX4 induced cell death. In this study, we further explore the relationship between DUX4 and HIF1α. We found that the DUX4 and HIF1α link differed according to the stage of myogenic differentiation and was conserved between human and mouse muscle. Finally, we found that HIF1α knock-down in an FSHD mouse model exacerbated DUX4-mediated muscle damages. Our data indicate that the suggested role of HIF1α in DUX4 toxicity is complex and that targeting HIF1α might be challenging in the context of FSHD therapeutic approaches.

Keywords: FSHD; DUX4; HIF1α

1. Introduction

FacioScapuloHumeral muscular Dystrophy (FSHD) is caused by the aberrant expression of the *DUX4* (DoUble homeoboX) gene in skeletal muscle **[1–3]**. However, the mechanisms leading from DUX4 protein expression to FSHD muscle structural and functional alterations are still unclear.

FSHD is a dominant hereditary disease primarily affecting skeletal muscle. It is characterized by a progressive and often left/right asymmetric skeletal muscle weakness that initially affects facial muscles, and progresses to shoulder girdle/proximal arm muscles, before reaching the lower body, especially lower limb muscles. FSHD does not impact life-span but drastically lowers quality of life, as approximately 30% of patients become wheelchair-bound by the age of 50 **[4,5]**. The early-onset infantile patients have higher morbidities and mortality because of faster disease progression and a higher rate of bulbar, respiratory, and cardiac involvement **[6]**. FSHD involves complex genetic and epigenetic components leading to activation in skeletal muscle of *DUX4*, a gene which codes for a potent transcription factor. DUX4 is normally expressed in germline and early embryogenesis, where it plays a role in zygotic genome activation and facilitates placentation **[7–9]**. In adults, DUX4 is normally silenced by DNA methylation except in mesenchymal stem cells, keratinocytes and thymus **[10,11]**. The genetic and epigenetic

 doi:10.20944/preprints202211.0532.v2

defect is located in the *4q35* chromosome region at the macrosatellite *D4Z4* repeat array, which is hypermethylated in healthy individuals and therefore in a closed chromatin conformation. FSHD results from the epigenetic derepression of the *D4Z4* repeat array, leading to its hypomethylation and thus, to a more permissive chromatin structure which allows *DUX4* gene transcription from the distal *D4Z4* unit **[2–4]**. Indeed, each *D4Z4* element contains the DUX4 promoter and ORF but lacks a polyadenylation signal (PAS): only transcripts from the distal *D4Z4* unit acquire an intron and a PAS by extension to the flanking *pLAM* region allowing for production of a stable *mRNA* that can express the toxic DUX4 protein. This PAS sequence is only present on the permissive distal 4qA allele, but not on 4qB **[12,13]**. FSHD was divided in two types based on their genetic causes. FSHD1 (95% of patients; OMIM #1589000) is linked to a partial deletion of the *D4Z4* repeat array (to 1 to 11 units) leading to epigenetic derepression and *DUX4* protein production from a 4qA allele. FSHD2 (5% of patients; OMIM #158901), has a digenic inheritance with (1) a less shortened D4Z4 array (from 12 to 20 units) on a 4qA allele and (2) a mutation in a gene involved in the epigenetic repression of the *D4Z4* repeats such as *SMCHD1*. A recent analysis of a large patient cohort suggests that FSHD1 and FSHD2 form a continuum of disease severity with increasing prevalence of genetic variants that affect epigenetic modifiers of the *D4Z4* array leading to a more open chromatin conformation **[14]**.

DUX4 encodes a potent transcription factor that has a causal role in FSHD pathophysiology **[1,3,17–20]**. Multiple pathways are affected in FSHD muscles and DUX4 likely operates in at least four different ways. First, despite its expression pattern in rare and short bursts, DUX4 transcriptional activity causes a drastic deregulation of gene expression leading to myogenesis defect, oxidative stress and cell death among other effects **[20]**. Several DUX4 direct target genes were identified in murine or human myoblasts and includes PITX1 **[3]**, germ-line specific genes **[17]** as well as genes involved in myogenesis **[21,22]** and oxidative stress response **[23–26]** (reviewed in **[20]**). Second, based on single cell RNA sequencing (sc-RNAseq) and microarray data, Banerji and Zammit have determined that repression of PAX7 target gene signature is a reliable biomarker of the pathology and is associated with disease progression **[4,21,22]**. PAX7 is a myogenic transcription factor normally expressed in satellite cells activated for regeneration, a process altered by DUX4 in FSHD. The single PAX7 homeodomain is similar to those of DUX4, and PAX7 can rescue DUX4-induced cytotoxicity in mouse **[23]**. DUX4 and PAX7 can bind similar DNA elements and compete on reporter target gene activation **[21]**. Third, through a concurrent RNAseq and quantitative proteomic study, Jagannathan et al. recently found a large discrepancy between the proteomic and transcriptomic landscapes in DUX4 expressing muscle cells. This highlighted the disturbance of post-transcriptional processes such as RNA and protein quality control pathways in DUX4-mediated deleterious effects in skeletal muscle cells **[27,28]**. Finally, another study hypothesized that DUX4 could, in addition to its transcriptional impact, interact with specific protein partners such as cytoplasmic desmin and RNA binding proteins that could consequently impact myogenesis **[29,30]**.

A molecular map of FSHD-associated interaction signaling based on a meta-analysis of microarray data sets from FSHD muscle biopsies have been published and constitutes a very useful tool to understand the FSHD pathophysiological mechanisms, and to guide therapeutic developments **[31]**. HIF1α signaling was described as critically perturbed in FSHD among other pathways such as WNT pathway. HIF1α is the central effector of the compensatory response to hypoxia. In FSHD, PAX7 repression was associated to the induction of hypoxia-response genes **[21].** Accordingly, Tsumagari et al. had independently described HIF1α-signaling network as one of the over-represented pathways among FSHD dysregulated genes **[32].** This pathway was further identified as necessary for DUX4 toxicity by Lek et al. who performed a genome-wide CRISPR-Cas9 screen to identify genes whose loss-of-function could allow survival of myoblasts

 doi:10.20944/preprints202211.0532.v2

expressing DUX4 **[33].** They showed that the use of pharmacological HIF1α signaling inhibitors could improve DUX4-associated muscle phenotypes in FSHD-like zebrafish models.

Given the numerous processes known to be influenced by HIF1α, and its link with DUX4, we wanted to investigate the cause and consequences of its aberrant expression in FSHD. HIF1α is the master regulator of physiological adaptive mechanisms in response to hypoxia **[34]**; it induces expression of multiple effector genes that modulate various cellular processes such as glucose metabolism and oxidative stress. In skeletal muscle, hypoxia modulates not only muscle fiber type profile but also myogenesis, regeneration and vascularization. Activation of HIF1α or HIF2α can also be involved in pathological conditions independently from hypoxia. This "pseudohypoxia" was mostly described in the field of cancer **[35]**. In FSHD, available data suggest that the primary genetic defect *per se* could be responsible for HIF1α pathway disturbance through a putative DUX4-HIF1α axis. In addition, as previously reviewed and discussed in **[36]**, it is important to note that additional causal mechanisms (hypoxemia resulting from respiratory insufficiency, ischemia caused by blood vessel abnormalities) could also participate in FSHD-associated dysregulation of HIF pathway in particular patient subgroups.

In the context of FSHD, it is important to note that HIF1α promotes a metabolic switch in favor of anaerobic glycolysis, the metabolism typically encountered in embryogenesis, where DUX4 and mouse Dux have a function in zygote genome activation **[7,8,37]**. Indeed, exposure of skeletal muscle cells to hypoxic conditions leads to HIF1α activation and subsequently to the up-regulation of 11 genes encoding for glycolytic enzymes **[38]**. Moreover, besides its effect on glycolysis, HIF1α reduces oxidative phosphorylation (OXPHOS) through the induction of pyruvate dehydrogenase kinase 1 (PDK1) **[39]**. PDK1 inactivates a subunit of pyruvate dehydrogenase (PDH) which metabolizes pyruvate at the mitochondrial membrane for entry into the tricarboxylic acid (Krebs) cycle **[40]**. Interestingly, most stem cell types reside in hypoxic niches where HIF1α controls pluripotency gene expression, promotes glycolytic metabolism and inhibits mitochondrial biogenesis. Since physiological DUX4 expression and function normally take place in the embryo, we can hypothesize that aberrant DUX4/HIF1α activation could contribute to metabolic disturbances in adult FSHD muscle cells. As mentioned above, HIF1α is known to modulate skeletal muscle differentiation and regeneration. Indeed activation of HIF1α by hypoxia exposure or by chemical activation was shown to have harmful effects on myogenic differentiation in murine muscle cells *in vitro* and delays or represses muscle regeneration after injury in mice (as we reviewed in **[41]**). Myogenic differentiation defects are a well know characteristic of FSHD. Indeed, FSHD myotubes display morphological features of aberrant differentiation leading to two major phenotypes: (**I**) myotubes with a thin, elongated morphology described as an hypotrophic (initially named "atrophic") phenotype; (**II**) myotubes displaying clusters of myonuclei and dysregulation of microtubule network, considered as 'disorganized' **[42,43]**. We therefore hypothesize that DUX4-induced HIF1α pathway misregulation could participate in FSHD-associated defect in adult myogenesis.

The present study aimed to decipher the causal link between DUX4 and HIF1α during early and late human muscle cell differentiation. We further studied DUX4-mediated HIF1α pathway changes in mature muscle with a murine model of local DUX4 expression we had previously developed [44]. Finally, through specific loss-of-function studies *in vivo*, we also investigated for the first time the effect of a targeted HIF1α knock-down on DUX4-mediated muscle lesion. We found that the link between DUX4 and HIF1α was conserved between human and mouse and depended on the myogenic differentiation

 doi:10.20944/preprints202211.0532.v2

stage. Interestingly, we showed that inhibiting HIF1α in a mouse model of DUX4 expression exacerbated DUX4 toxicity suggesting that targeting the DUX4-HIF1 α axis is trickier than expected in the context of a therapeutic approach for FSHD.

2. Results

2.1. Effect of DUX4 expression on HIF1α protein level in myoblasts and myotubes in vitro

We used the genetically-engineered human LHCN-M2-iDUX4, myoblast line with doxycycline (DOX)-inducible DUX4 expression, engineered from the immortalized human myoblast line LHCN-M2 **[45,46]**. DUX4 induction was first evaluated by the resulting cell toxicity determined using MTT and CCK8 viability assays 24h after DOX addition. These tests were performed in LHCN-M2-iDUX4 myoblasts (**Figure S1B and D**) as well as on LHCN-M2 to test DOX toxicity *per se* (**Figure S1A and C**). DUX4 induction had no effect on cell viability up to 62.5 ng/ml DOX. From 125 ng/ml and above, a significant decrease of viability was observed in both the MTT and CCK8 tests (**Figure S1B and D**). DOX exposure *per se* had no effect on myoblast viability in the absence of DUX4 expression as verified in LHCN cells (**Figure S1A and C**). The production of the DUX4 protein was also checked by immunofluorescence (IF) in LHCN-M2-iDUX4 myoblasts (**Figure S1E**). At 15.6 and 31.2 ng/ml, we detected 32% (± 4%) and 56% (± 6%) of DUX4-positive (DUX4$^+$) nuclei, respectively. Between 62.5 ng/ml and 250 ng/ml of DOX, we detected up to 80% of DUX4$^+$ nuclei but this percentage was not significantly different among these higher doses. The dose of 62,5 ng/ml of DOX was therefore selected for further experiments because it showed the best DUX4 induction with no effect on cell viability.

The impact of DUX4 on *HIF1α mRNA* and protein level was then studied in LHCN-M2-iDUX4 myoblasts in proliferation (myoblasts), as well as in early (myocytes) and late (myotubes) differentiation stages. DUX4 expression nearly halved the proportion of HIF1α-positive (HIF1α^+) nuclei in proliferating myoblasts (**Figure 1A-C**) with control cells presenting 44 % (± 3%) of cells with nuclear HIF1α^+ nuclei but only 26% (±5%) of HIF1α^+ nuclei with DUX4. Accordingly, *HIF1α mRNA* level was halved in proliferating myoblasts expressing DUX4 (**Figure 1D**). In myocytes, the percentage of HIF1α^+ nuclei strongly trended toward a decrease without reaching the statistical significance (p=0.051, t-test) (**Figure 1E-G**) and *HIF1α* expression was not significantly modified at the *mRNA* level (**Figure 1H**). In myotubes, the percentage of HIF1α^+ nuclei doubled upon *DUX4* induction (31% ±5%) compared to uninduced controls (16%±4%)(**Figure 1I-K**). Concomitantly, *HIF1α mRNA* level was significantly increased (**Figure 1L**). Intriguingly, only 48% of HIF1α^+ nuclei presented DUX4 immunofluorescence staining (**Figure 1M-N**).

2.3. Effect of DUX4 expression on HIF1α pathway in vitro

To further determine the impact of DUX4 on the HIF1α pathway, we studied the effect of *DUX4* expression on two direct HIF1α transcriptional targets: *VEGF* and *PDK1*. *PDK1 mRNA* level was decreased twofold in proliferating myoblasts expressing DUX4 ($p<0.01$, T-test), but *VEGF mRNA* level was not significantly modified as compared to non-induced cells (**Figure 2A**). In agreement with our results obtained at the *RNA* level, western blotting showed a significant decrease of PDK1 protein abundance in proliferating myoblasts after DOX induction (**Figure 2B-C**). In myocytes expressing DUX4, the *mRNA* level of both HIF1α target genes was not significantly modified (**Figure 2D**) but PDK1 protein relative abundance was reduced, as observed in myoblasts (**Figure 2E-F**). In myotubes, similarly to the results obtained for HIF1α, the *mRNA* level of its target genes *PDK1* and *VEGF* were significantly increased 3- and 4-fold, respectively (**Figure 2G**). However, surprisingly, PDK1 protein level was significantly decreased upon DUX4 expression ($p<0.01$, T test; **Figure 2H-I**).

Preprints (www.preprints.org) | NOT PEER-REVIEWED | Posted: 5 December 2022 doi:10.20944/preprints202211.0532.v2

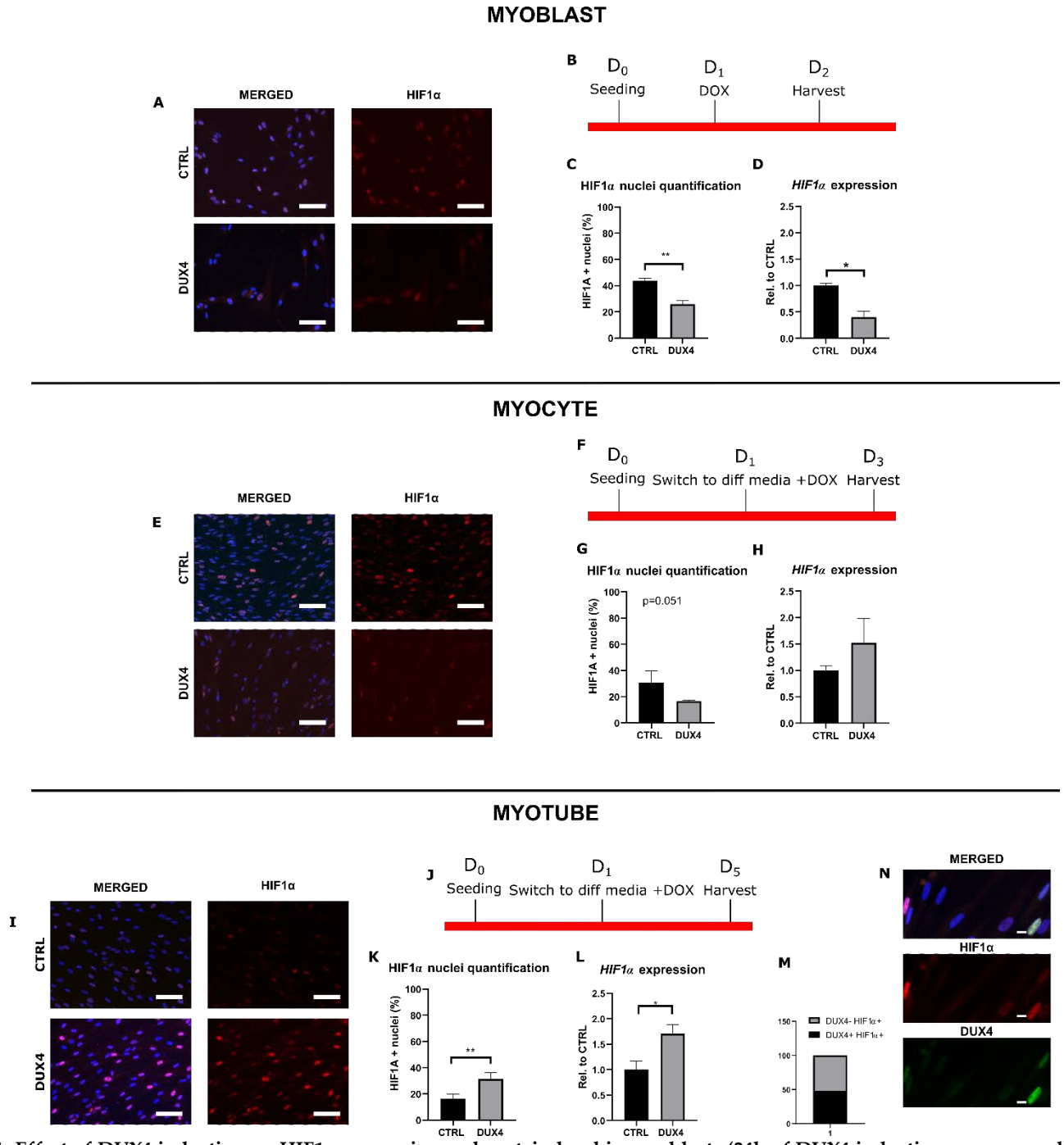

Figure 1. Effect of DUX4 induction on HIF1α expression and protein level in myoblasts (24h of DUX4 induction; upper panel), myocyte (48h of DUX4 induction; middle panel) and myotubes (48h of DUX4 induction; lower panel). Differentiation was induced for two (myocytes) or four days (myotubes) after the cells reached 100% confluence. Cells were fixed in 4% PAF and incubated with HIF1α antibody and a secondary antibody coupled to Alexa Fluor (red). **A-E-I.** Representative fields showing HIF1α positive (HIF1α⁺) nuclei detected by immunofluorescence (red). DAPI was used to visualize nuclei (blue). Scale bar= 100µm. **B-F-J**. Experiment time courses. **C-G-K.** Quantification of HIF1α⁺ nuclei normalized to the total number of nuclei (DAPI). N=3, mean ± SEM, **p<0.01, T-test. **D-H-L.** Relative *HIF1α* mRNA level normalized to *RPLP0* RNA (RT-qPCR, see Methods). N=4 for myoblasts, N=3 for myocytes and myotubes; mean ± SEM, *p<0.05, **p<0.01, T-test**. M.** Proportion of DUX4⁺ nuclei among HIF1α⁺ nuclei. **N**. Representative field showing HIF1α⁺ (red) and DUX4⁺ (green) staining by immunofluorescence. DAPI was used to visualize nuclei (blue). All experiments were performed on 3 independent cultures, each at least in triplicate.

Preprints (www.preprints.org) | NOT PEER-REVIEWED | Posted: 5 December 2022 doi:10.20944/preprints202211.0532.v2

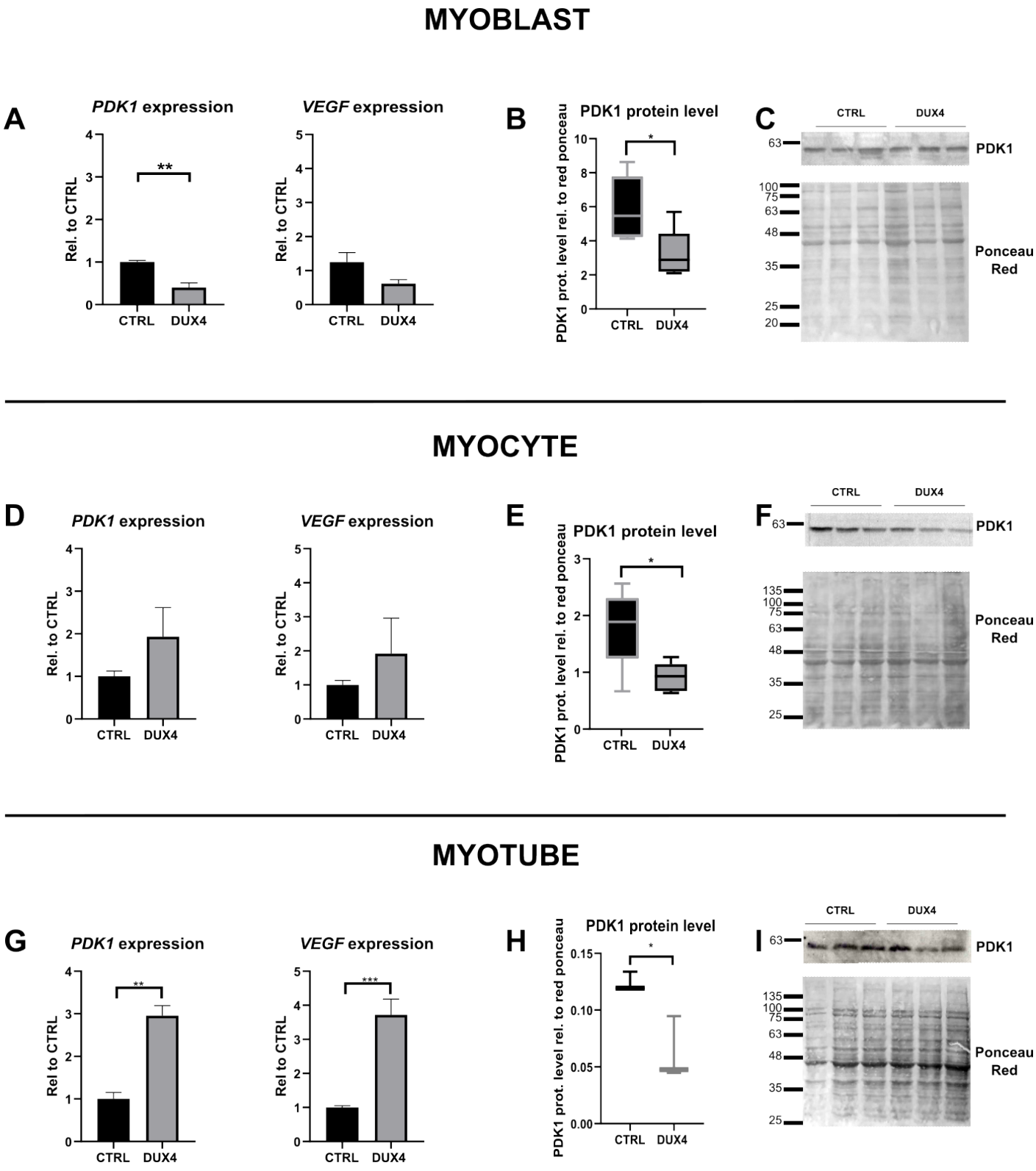

Figure 2. Effect of DUX4 induction on HIF1α target genes in myoblasts (24h of DUX4 induction; upper panel), myocytes (48h of DUX4 induction; middle panel) and myotubes (48h of DUX4 induction; lower panel). A-D-G. Relative levels of *PDK1* and *VEGF* mRNAs quantified by RT-qPCR and normalized to *RPLP0* RNA. N=4 for myoblasts, N=3 for myocytes and myotubes; mean ± SEM, *p<0.05, **p<0.01, ***p<0.001, T-test. **B-E-H.** PDK1 protein level determined by Western blot. Densitometry signal was normalized to total protein stained by Ponceau red. N=6 for myoblast and myocytes, n=3 for myotubes, *p<0.05, Rank sum test for myoblasts and myocytes, and T-test for myotubes. **C-F-I.** Representative Western blot for PDK1 detection in LHCN-M2-iDUX4 cells induced with 62.5 ng/mL doxycycline for 24h and Ponceau red staining.

 doi:10.20944/preprints202211.0532.v2

2.4. Effect of DUX4 on HIF1α expression in mouse myoblasts

Since many DUX4-mediated signaling alterations were conserved between human and mouse **[31]**, we investigated whether the effect of DUX4 expression on HIF1α *mRNA* level observed in human myoblasts was conserved in murine muscle cells. To this aim, we used iC2C12-DUX4 cells derived from mouse C2C12 myoblasts and harboring a DOX-inducible DUX4 gene **[23]**. LHCN-iDUX4 and iC2C12-DUX4 were both induced using increasing DOX doses. In both cell lines, DUX4 expression decreased the proportion of HIF1α⁺ nuclei. However, the basal level of HIF1α⁺ nuclei in mouse myoblasts was higher than in human myoblasts. Indeed, human myoblasts displayed 44% (± 3%) of HIF1α⁺ nuclei while mouse myoblasts presented 73% (± 4%) of HIF1α⁺ nuclei (**Figure 3**). Moreover, in human myoblasts, low doses of DOX were sufficient to decrease the percentage of HIF1α⁺ nuclei. Indeed, at the dose of 15.6 ng/ml of DOX, a significant decrease of the number of HIF1α⁺ nuclei was observed ($p<0.001$, One Way ANOVA), while in mouse myoblast, the reduction of HIF1α⁺ nuclei could only be seen from 31.2 ng/ml of DOX ($p<0.01$, One Way ANOVA) (**Figure 3**).

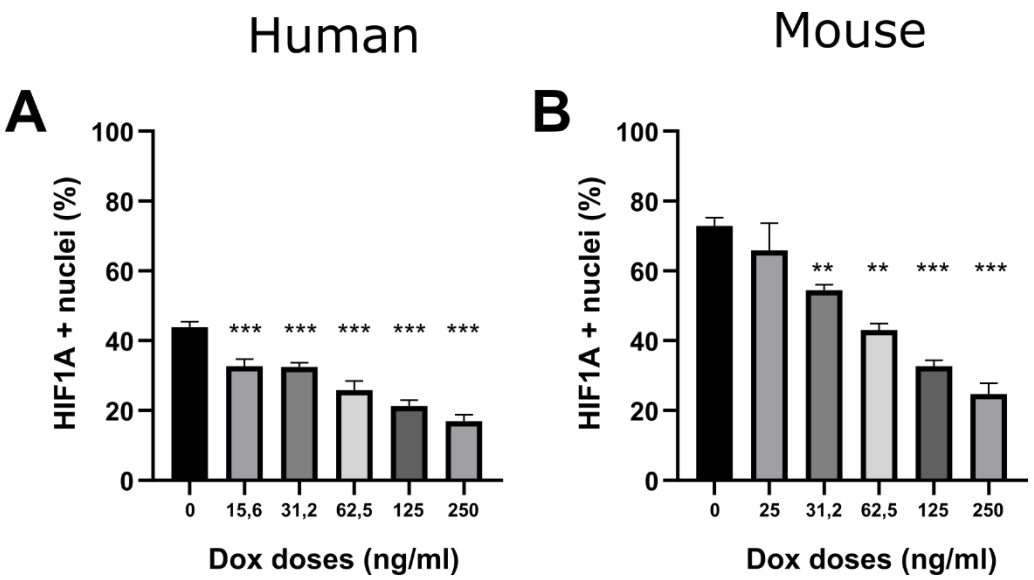

Figure 3. Effect of DUX4 on the number of HIF1α-positive nuclei (HIF1α⁺) in mouse *vs* human myoblast. 200 000 cells were seeded per well in 6-well plates and induced for 24 h with increasing doses of doxycycline (DOX, ng/ml). HIF1α was detected by immunofluorescence (IF). **A.** Quantification of HIF1α⁺ nuclei normalized to the total number of nuclei (DAPI staining) in LHCN-iDUX4 myoblasts. Mean ± SEM, ***p<0.01, One way ANOVA with Holm Sidak post hoc test vs the control (DOX : 0 ng/ml). **B.** Quantification of HIF1α⁺ nuclei normalized to the total number of nuclei (DAPI) in iC2C12 myoblasts. Mean ± SEM, **p<0.01, *** p<0.001, One way ANOVA with Holm Sidak post hoc test *vs* the control (DOX : 0 ng/ml). The experiments were performed on 3 independent cultures, each in triplicate (n=3).

2.5. Effect of DUX4 expression on the HIF1α pathway in a murine model in vivo

To investigate the potential link between DUX4 and the HIF1α pathway in a mature muscle *in vivo*, we used the DUX4 IMEP model we had previously developed **[44]**. In this model, a DUX4 expression plasmid (*pCIneo-DUX4*) is injected in the *Tibialis Anterior* (TA) hindlimb muscle followed by electroporation (IMEP) leading to local DUX4 expression and myopathy. First, a dose–response analysis was performed with increasing doses of *pCIneo-DUX4*, using the backbone control plasmid (*pCIneo*) or a saline solution as negative controls. TA muscles were harvested 7 days post IMEP, embedded and frozen. Cryosections were stained using Hematoxylin-Eosin-Heindehain blue staining (HEB). The quantification of muscle damage characterized by extracellular matrix expansion and hypotrophic myofibres was reported to total muscle section and performed as described

Preprints (www.preprints.org) | NOT PEER-REVIEWED | Posted: 5 December 2022 doi:10.20944/preprints202211.0532.v2

in **[44]**. However, at 14 and 21 days after *pCIneo-DUX4* electroporation, the TA muscle of DUX4-IMEP mice no longer exhibited these histological features but presented many fibers with centrally located nuclei suggesting muscle regeneration (**Figure 4A**). Upon quantification of the damaged area, we found no statistical difference between the saline and the *pCIneo* control plasmid groups, therefore, we pooled data from both groups into a single control group. The lowest *pCIneo-DUX4* dose causing a significant increase of the damaged area (median of 20%) compared to the control group (median of 7%) was 5µg ($p<0.05$, ANOVA on Ranks followed by Dunn's post hoc test; **Figure 4A** and **B**). To check DUX4 biological activity, we quantified the *mRNA* level of its mouse target gene *Wfdc3*. We found no statistical difference in *Wfdc3 mRNA* level between the saline and the *pCIneo* control plasmid groups, therefore, we pooled data from both groups into a single control group. A significant increase in *Wfdc3 mRNA* level was detected by RT-qPCR at days 1, 3, 7 and 14 post-injection, confirming DUX4 expression in the injected TA (**Figure 4C**). However, we could not detect the increase of *Wfdc3 mRNA* level anymore at 21 days post-injection. We then investigated *Hif1α* pathway alterations in this model at 1, 3, 7 and 14 days post-injection. No significant difference was detected in *Hif1α mRNA* level and its target gene *Pdk1* regardless the timepoint. However, at one day post-injection, a significant increase of *Vegf mRNA* level was observed in the control mice injected with *pCIneo* as compared to saline. This increase was not detected with *pCIneo-DUX4* injection (**Figure 4D**).

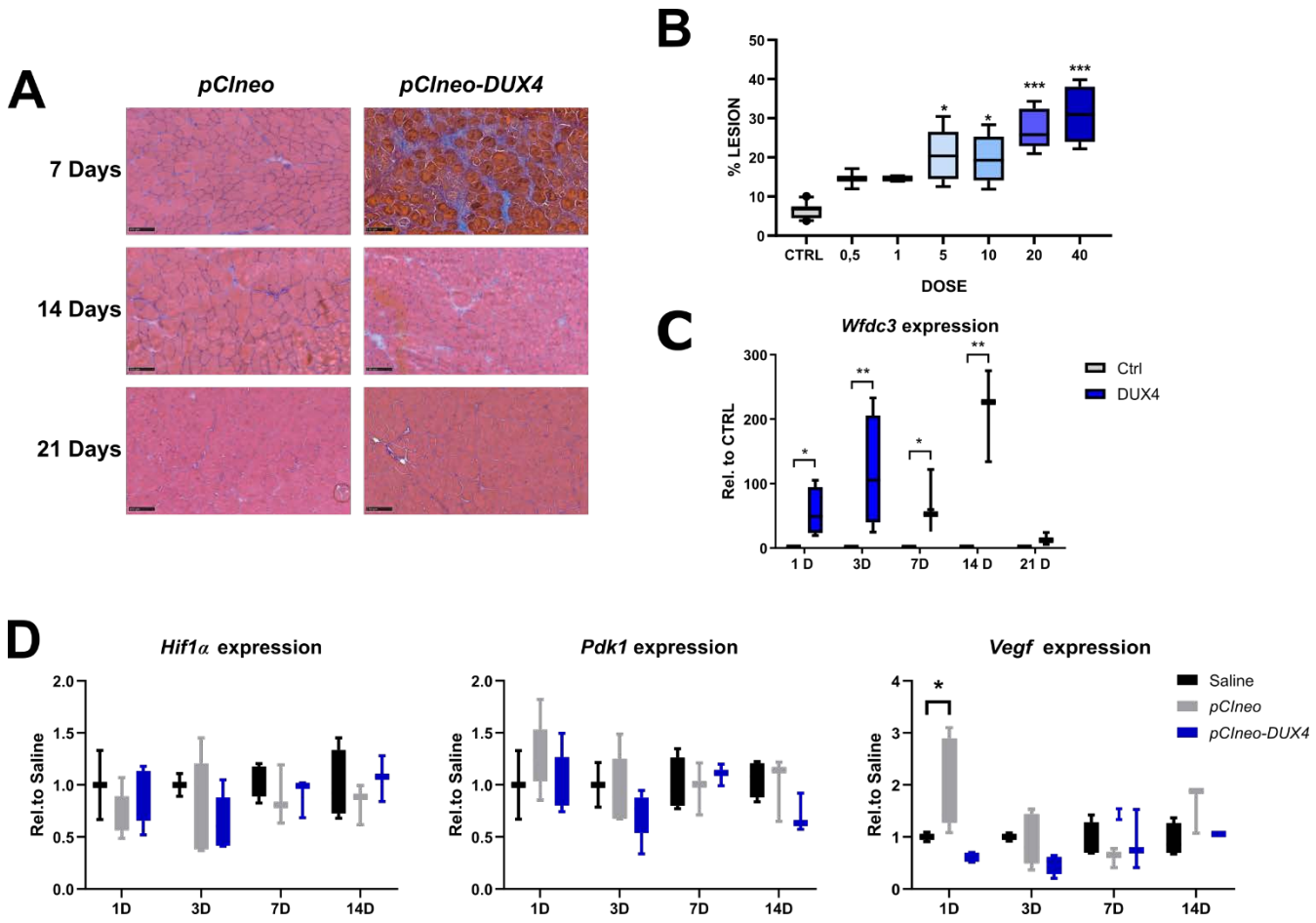

Figure 4. Effect of DUX4 induction on *Hif1α* pathway in the DUX4 IMEP murine model used with a low dose of DUX4 expression plasmid. A. Representative sections of TA electroporated with 5 µg of (left column) *pCIneo* or (right column) *pCIneo-DUX4* plasmids at 7-, 14- and 21-days post-injection**.** Scale = 100µm. **B.** Dose–response of plasmid amount *vs* muscle lesion area in mouse TA, 1-week post IMEP procedure. Lesion area percentage was evaluated on total cryosection of medial and proximal part of TA electroporated with different doses of a DUX4-expression plasmid (*pCIneo-DUX4*). Results obtained from saline solution injected groups and *pCIneo* group were pooled into a single control group, as no statistical difference could be highlighted between groups whatever time points. * p< 0,05, ** p< 0,01, ***p<0,001, Kruskal Wallis followed by Dunn's post hoc test. Control group n=10, 0,5 µg and 1µg n=2, 5µg n=6,

10 µg n=7, 20µg n=8, 40µg n=4. **C.** Effect of DUX4 induction on *Wfdc3 mRNA* level in the IMEP model. Expression is normalized to *Rplp0* RNA, * p< 0,05, ** p< 0,01; Kruskal Wallis followed by a Dunn's post-hoc test. For 1- and 3-day group: *pCIneo-DUX4* n=4, *pCIneo* n=6, saline n=2. For 7- and 14-day groups: *pCIneo-DUX4* n=3, *pCIneo* n=3, saline n=4. For the 21-day group: *pCIneo-DUX4* n=3, *pCIneo* n=4, saline n=4. Results obtained from saline solution injected groups and *pCIneo* group were pooled into a single control group, as no statistical difference could be highlighted between groups whatever time points. **D.** Effect of DUX4 induction on *Hif1α mRNA* level in the IMEP model. Expression is normalized to *Rplp0* gene. *p< 0,05, **p< 0,01; Kruskal Wallis followed by a Dunn's post-hoc test. For 1- and 3-day group: *pCIneo-DUX4* n=4, *pCIneo* n=6. For 7- and 14-days group: *pCIneo-DUX4* n=3, *pCIneo* n=4. For the 21-day group: *pCIneo-DUX4* n=3, *pCIneo* n=4. Results obtained from saline solution injected groups from all time points, were pooled together, as no statistical difference could be highlighted between groups whatever time points for all tested genes, saline group n=14.

In contrast to the data that we obtained in human myoblasts and myotubes, DUX4 expression did not affect the *HIF1α* pathway in mouse adult myofibers in the DUX4 IMEP model at the investigated time post injection and by using a 5-µg dose of DUX4 expression plasmid. The first hypothesis that would explain those divergent results was that DUX4 could influence the HIF1α pathway in human but not in murine muscle cells. However, we have shown that DUX4 could decrease the number of HIF1α$^+$ nuclei in murine as well as in human myoblasts (**Figure 3**). We therefore investigated whether HIF1α dysregulation could constitute an early event following DUX4 expression. To this aim, and to respect the ethical principle of reduction of animal experimentation, we first selected the most relevant acute timepoints in a model *in vitro*. C2C12 murine myoblasts were transfected with *pCIneo-DUX4* because this method was closer to the conditions used in the DUX4 IMEP model *in vivo* as compared to DUX4 inducible cell models (**Figure 5B**). To evaluate the kinetic of DUX4 target gene transcription following the transfection, we quantified, by RT-qPCR, the *mRNA* levels of two DUX4 target genes, *Wfdc3* and *Zscan4*. We could detect a significant increase of *Zscan4* expression at 5h and 6h post transfection of 4- and 17-fold, respectively. There was also an 8-fold increase in *Wfdc3 mRNA* level at 6h only. The *Hif1α* pathway was therefore investigated at these timepoints in the DUX4 IMEP model. To increase the model sensitivity, we also increased the dose of *pCIneo-DUX4* up to 20µg to detect a highly significant (compared to 5µg) increase of the muscle lesion area (median of 26%) (p<0.001, ANOVA on Ranks followed by Dunn's post hoc test; **Figure 5A** and **4B**). At 6h, 1 day and 7 days post-injection, a significant increase of *Wfdc3 mRNA* was detected, confirming DUX4 expression in the injected TA (**Figure 5C**). Concerning *Hif1α mRNA* level, an increase was observed in TA 6h after injection of *pCIneo-DUX4* and *pCIneo*. At 1 day post injection, *Hif1α* expression was only increased in the *pCIneo-DUX4* group, as compared to the control groups injected with the *pCIneo* plasmid or the saline solution. However, the expression of target genes *Pdk1* and *Vegf* was not significantly modified whatever experimental group and time point (**Figure 5D**).

2.7. Contribution of Hif1α to the developpement of muscle lesions induced by DUX4.

Since DUX4 deregulated *Hif1α mRNA* level in mouse TA muscle, we determined the involvement of Hif1α in DUX4-mediated muscle damages *in vivo* through loss-of-function experiments by using siRNAs targeting *Hif1α* transcripts (*siHIF1α*) in the DUX4 IMEP model. We first checked s*iHIF1α* efficiency through a dose response analysis and found that 2µg of *siHIF1α* allowed a significant twofold downregulation of *Hif1α mRNA* level as compared to the TA injected with the control siRNA (*siCTL)* or saline (**Figure 6A**). To evaluate the implication of Hif1α in muscle lesions induced by DUX4, we used as outcome measure the global quantification of the damaged surface area in the TA muscle in the DUX4 IMEP model at 7 days. The *pCIneo-DUX4* DNA was injected alone or in combination with 2µg *siCTL* or *siHIF1α* (**Figure 6B**). A significant 10% increase of muscle lesion area was observed in the *siHIF* group, as compared to the s*iCTL* and saline groups (**Figure 6C**). The muscle damage of the *siHIF* group was characterized by extracellular matrix expansion (as shown by HEB staining), and increased number of smaller fibers.

Preprints (www.preprints.org) | NOT PEER-REVIEWED | Posted: 5 December 2022 doi:10.20944/preprints202211.0532.v2

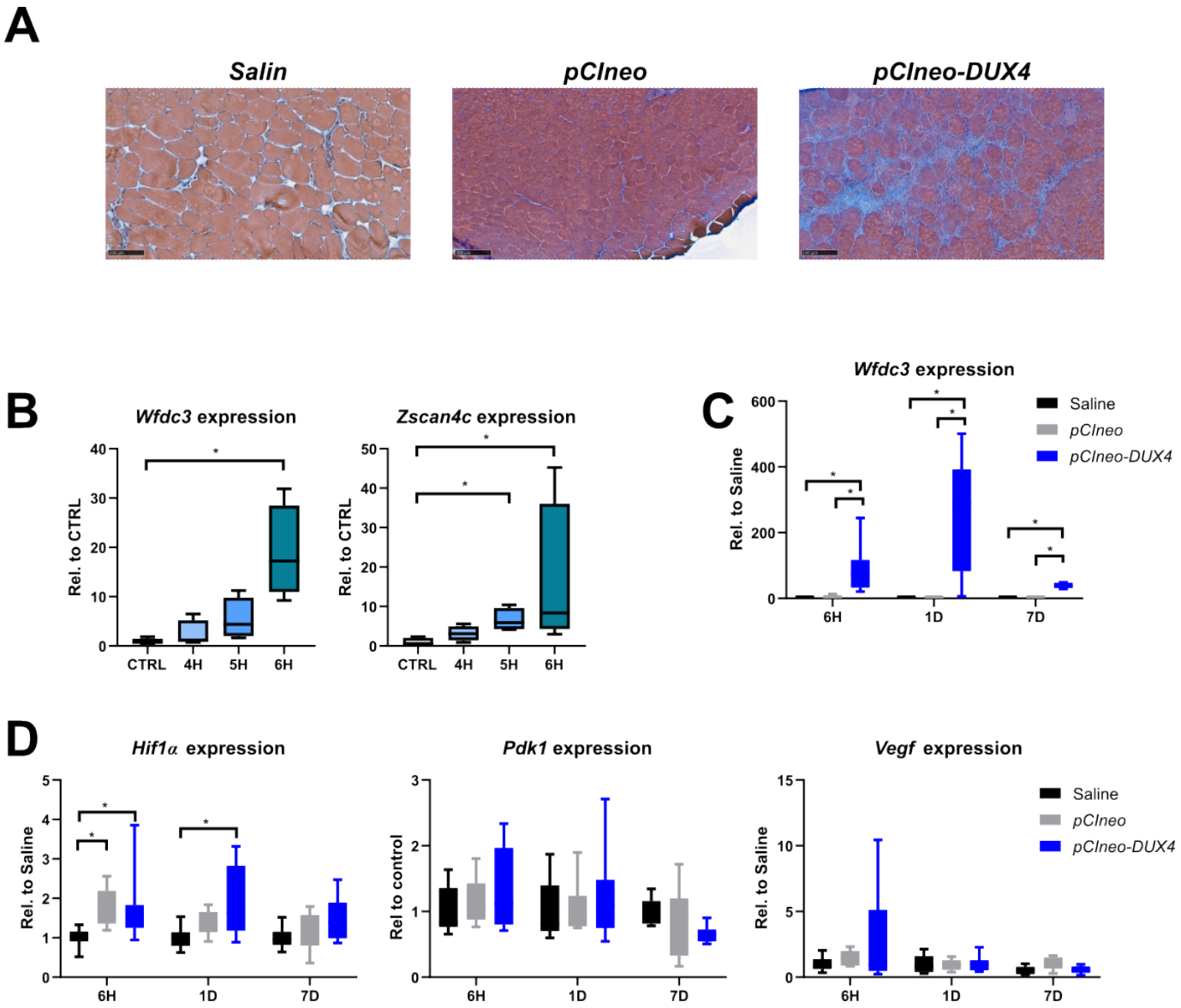

Figure 5. **Early effects of DUX4 expression on HIF1α pathway *in vivo* in the DUX4 IMEP mouse model with a high dose of DUX4 expression plasmid**. **A**. Representative sections of TA electroporated with saline solution (Left), 20 µg of *pCIneo* (Middle) or *pCIneo-DUX4* plasmid (Right)**.** Scale = 100µm**. B.** RNAs of DUX4 target genes, *Wfdc3* and *Zscan4* were quantified by RT-qPCR in C2C12 myoblasts 4, 5 and 6h post transfection with *pCIneo-DUX4*. *mRNAs* were normalized to *Rlpl0* RNA. Kruskal Wallis followed by a Dunn's post-hoc test, * p<0.05. N=5 for control group and n=4 for 4h, 5h, and 6h group. **C.** Effect of DUX4 induction on *Wfdc3* mRNA level was quantified by RT-qPCR in the IMEP model. *mRNA* levels were normalized to *Rplp0* RNA. Kruskal Wallis followed by a Dunn's post-hoc test, *p<0.05. N=8. **D.** Effect of DUX4 induction on Hif1α pathway in the IMEP model. mRNA levels were normalized to *Rplpl0* RNA. Kruskal Wallis followed by a Dunn's post-hoc test, *p<0.05. N=8 for each group.

Preprints (www.preprints.org) | NOT PEER-REVIEWED | Posted: 5 December 2022 doi:10.20944/preprints202211.0532.v2

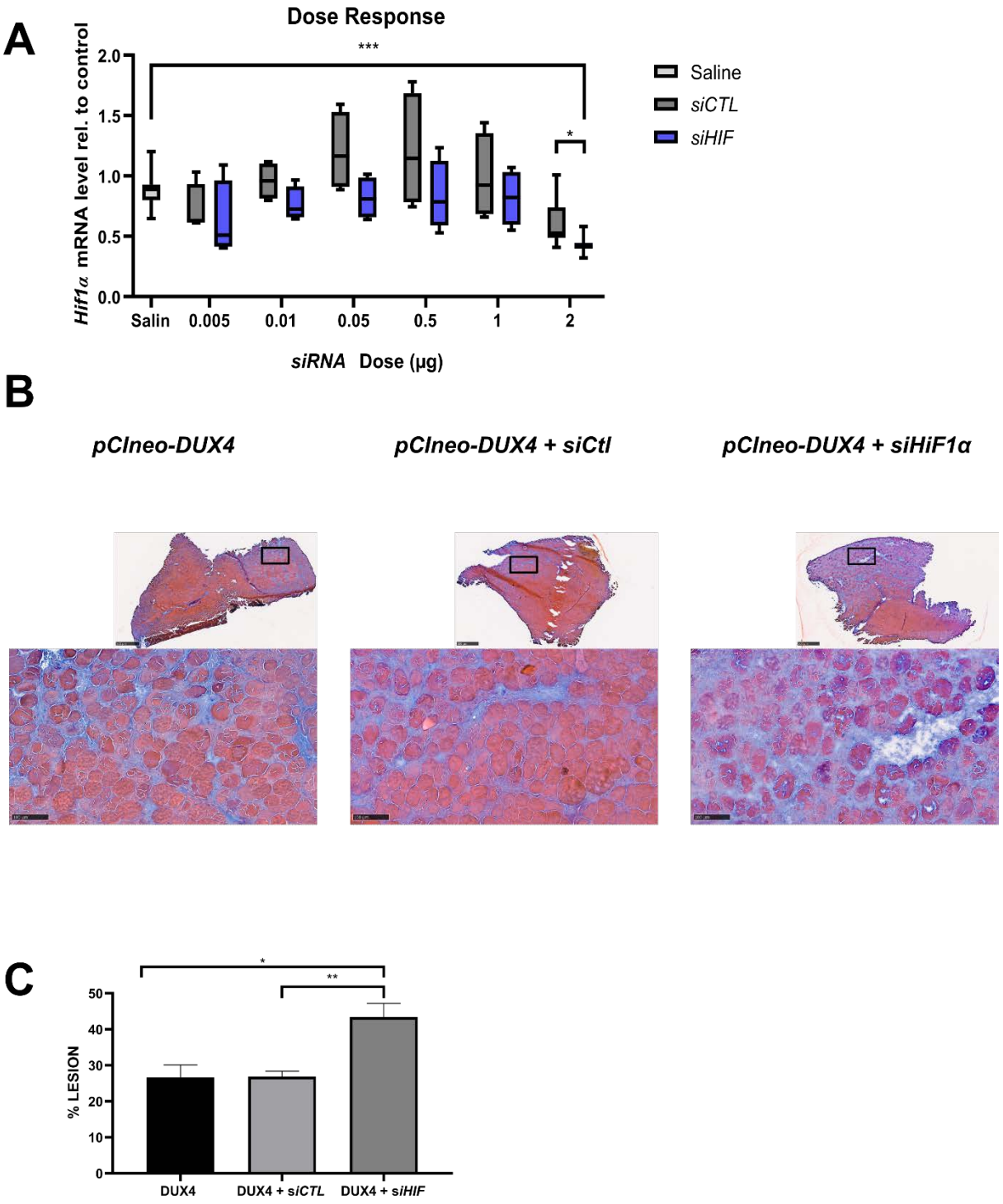

Figure 6. Involvement of HIF1α pathway in DUX4-induced muscle damages. A. The efficiency of siRNA directed against *Hif1α mRNA* (*siHIF*): dose response analysis. The TA muscle was electroporated with either saline solution, *siCTL* or *siHIF*. *Hif1α mRNA* level was quantified by RT-qPCR and normalized to *Rplp0* RNA. *p<0.05, **p<0.01, Kruskal Wallis followed by a Dunn's post-hoc test. Saline n=10, 0.005 µg, 0.01 µg, 0.05 µg, 0.5 µg and 1 µg n=4, 2µg n=10. **B.** Representative cryosections of TA electroporated with 20 µg of *pCIneo-DUX4* plasmid in combination or not with 2µg of *siCTL* or *siHIF*. Muscle sections were stained with HEB. **Top**: global view of the muscle sections; Scale = 500µm. **Bottom**: magnification of the damaged area; Scale = 100µm. **C.** Percentage of lesion area was evaluated on muscle stained with HEB as represented in B. Mean ± SEM, *p<0.05, **p<0.01, One way ANOVA followed by Holm-Sidak post-hoc test. N=4 for each group.

 doi:10.20944/preprints202211.0532.v2

3. Discussion

DUX4-induced HIF1 pathway disturbances depend on the differentiation state of human muscle cells.

The HIF1α signaling pathway was described as critically disturbed in FSHD muscles **[21,31]** and as a key driver of DUX4-induced myoblast death **[33]**. In the present study, we confirmed that HIF1α nuclear protein level was altered in human muscle cells upon DUX4 expression. However, we discovered that these alterations depended on the stage of myogenic differentiation. Indeed, in proliferating myoblasts, HIF1α was downregulated at the *mRNA* and protein level upon DUX4 expression but in contrast, DUX4 expression induced HIF1α and its pathway in myotubes. At the intermediate differentiation stage (myocytes), HIF1α expression was not significantly modified by DUX4 expression. Previous data had suggested that DUX4-mediated cell death required induction of the HIF1α pathway in another model of DUX4 inducible myoblast (iDUX4-MB135). Indeed, Lek *et al.* showed that HIF1α protein stabilization and nuclear localization upon DUX4 expression as well as a colocalization of HIF1α in nuclei with high DUX4 expression suggesting that a threshold of DUX4 expression was necessary to trigger HIF1α stabilization **[33]**. In our study, this positive relationship was observed in DUX4-expressing LHCN-M2 myotubes, but not in proliferating myoblasts. The use of different muscle cell line is not expected to strongly influence the DUX4/HIF1α axis, contrarily to culture conditions. Indeed, addition of dexamethasone to the culture medium (as per Lek *et al.)* was found to lower DUX4 expression in FSHD myoblasts **[47]**. Similarly, dexamethasone treatment of human myoblasts for 24h decreased expression of *VEGF*, a HIF1α target gene **[48]**. Therefore, in our study, we cultured myoblasts in a medium lacking dexamethasone, based on the original publication which described the inducible LHCN-M2-iDUX4 cell line **[24]**.

The different regulation of HIF1α upon DUX4 expression in myoblasts and myotubes could partly be explained by distinct basal levels of HIF1α according to the differentiation stages. Indeed, basal Hif1α protein level was shown to be higher in murine myoblasts compared to myotubes. This is unlikely due to different gene expression levels since no change in *mRNA* abundance was seen **[49]**. Interestingly, *Hif1α RNA* silencing or protein chemical inhibition by echinomycin in mouse muscle cells caused (**I**) a downregulation of the nuclear translocation of MyoD, a transcription factor activated during myoblast differentiation (**II**) and decreased *Myogenin* and *Myosin heavy chain (Myhc)* expression, ultimately leading to reduction of myoblast fusion and differentiation indices **[50]**. On the other hand, C2C12 myotubes treated with $CoCl_2$, a chemical activator of HIF1α protein, exhibited an increase in the autophagy and atrophy pathways **[51]**. Moreover, DUX4 impairs myogenic differentiation in human **[24]** or mouse myoblasts **[23]**. Several studies (transcription profiles and fusion index) with FSHD muscle cells have shown that myogenesis was impaired **[4,21,24,32,43,52]**. In aggregate, these data suggest that the inhibition of *HIF1α* in myoblasts and the activation of *HIF1α* in myotubes by DUX4 could both contribute to the myogenesis defect observed in FSHD.

In myotubes, we observed that only half of HIF1α$^+$ nuclei co-expressed DUX4. This suggested a particular kinetic between DUX4 expression and activation of HIF1α production and nuclear translocation. Direct or indirect mechanistic hypotheses might be suggested: (**I**) a direct DUX4-mediated transcriptional regulation of the gene encoding HIF1α. As described in **[53]**, the expression dynamics and an asynchronous regulation of DUX4 and HIF1α half-life could explain why both proteins were detected either individually in separate nuclei or together in identical nuclei. (**II**) DUX4 could activate HIF1α pathway in satellite cells by disturbing the ability of PAX7 to regulate its transcriptional network **[21]**. (**III**) HIF1α could also be stabilized by Reactive Oxygen Species (ROS) through an inhibi-

 doi:10.20944/preprints202211.0532.v2

tion of prolyl hydroxylase enzymes (PHD) activity **[54]**. Indeed, several clinical and experimental studies point to the involvement of an excessive oxidative stress in FSHD **[25,52,55–59]** (As reviewed in [60]). A recent study also showed high mitochondrial ROS in FSHD myogenic cells **[25]**. Thus, DUX4 could cause generation of ROS that should be able to stabilize HIF1α protein even in nuclei that do not express DUX4.

We also further investigated the effect of DUX4 on the HIF1α pathway through the analysis of its target gene expression. *VEGF* and *PDK1* were globally repressed in proliferating human myoblasts, unchanged in myocytes and induced in myotubes expressing DUX4. In proliferating myoblasts expressing DUX4, PDK1 protein abundance was reduced together with its *mRNA* level. However, in myocytes and myotubes, PDK1 protein abundance was further decreased upon DUX4 expression, suggesting a post-translation regulation potentially involving additional factors, some of which could be independent of HIF1α transcriptional activity. The opposite effects we observed for *VEGF* and *PDK1* RNA levels in myoblasts (repression) versus myotubes (induction), together with the intermediate HIF1α-PDK1 pathway regulation shown in myocytes expressing DUX4, suggested a transition occurring during the differentiation process. Since HIF1α is a master regulator of the cell response to alterations in oxygen levels, its sustained stabilization in skeletal muscle might affect muscle mass through metabolic disturbances or an increased sensitivity to oxidative stress, a major feature of FSHD. Exposure of skeletal muscle cells to hypoxic conditions leads to HIF1α activation and the subsequent up-regulation of genes encoding enzymes that promote a glycolytic metabolism **[38]**. It is well established that most stem cell types reside in hypoxic niches where HIF1α controls pluripotency gene expression, promotes glycolytic metabolism and inhibits mitochondrial biogenesis. However, when myoblasts differentiate and fuse into multinucleated myofibers, a reconfiguration of metabolic programs toward OXPHOS occurs, especially via an increased mitochondrial biogenesis and activity [61]. DUX4 was shown to disturb this process via its target gene activation and repression to orchestrate a transcriptome characteristic of a less-differentiated cell state [62]. Moreover, HIF1α is expressed in the embryo and it known to protect it from intrauterine hypoxia and regulates its metabolism [63]. Therefore, since DUX4 expression activates embryonic genes, and the embryo metabolism is glycolytic, we can hypothesize that an abnormal activation of glycolysis through HIF1α could contribute to metabolic disturbances in FSHD muscle cells. Evidence for mitochondrial dysfunction was found in FSHD muscle where impaired energy metabolism was linked to alterations in mitochondrial ultrastructure and subsarcolemmal and intramyofibrillar distribution **[55]**. Furthermore, a dynamic transcriptomic analysis identified that suppression of PGC1α/ ERRα axis, a critical component of the mitochondrial biogenesis pathway, was associated to the myogenesis defect in FSHD **[42]**. Recently, transcriptomic data from FSHD muscle showed enrichment for disturbed mitochondrial pathways. The alteration of mitochondrial ROS metabolism was correlated with mitochondrial membrane polarization and myotube hypotrophy phenotype. DUX4-induced modifications in the mitochondrial function occurred before mitochondrial ROS generation and affected hypoxia signaling via complex I **[25]**. These observations could also explain the decreased PDK1 protein level observed in our study since this metabolic regulator is mainly located in the mitochondria [64]. Therefore, mitochondrial dysfunction along with the DUX4-mediated mitochondrial ROS production could lead to *PDK1* post-transcriptional deregulation e.g. protein degradation through the proteasome or autophagy process [65]. DUX4-HIF1α-VEGF pathway disturbances observed in the present study also depend on the differentiation stage of muscle cells. Even if this axis alone was likely not sufficient to explain all the pathological features of FSHD muscle, it might be important to further explore the role of HIF1α since an histopathological study of patient muscle biopsies has indicated a decrease of capillary density [66]. Interestingly, it has been shown that there was an impaired oxygen demand during exercise in FSHD and that lower oxygen consumption was related

 doi:10.20944/preprints202211.0532.v2

to oxidative stress **[57]**. Moreover, patients affected with infantile FSHD can present exudative retinopathy due to retinal telangiectasias [67–69]. In this context, HIF1α could constitute an interesting candidate to better understand FSHD-associated vasculopathy.

The DUX4/HIF1a axis is conserved in murine in vitro and in vivo models.

Our data also indicate that the DUX4-HIF axis highlighted in human muscle cells is similarly observed in murine myoblasts and mature muscle in mice. This point is of interest because most therapeutic strategies need testing *in vivo* in preclinical model. Here, we investigated the DUX4/HIF1α axis *in vivo* in the DUX4-IMEP model in which a DUX4 expression plasmid is injected and electroporated into the TA muscle, inducing a dose-dependent local myopathy. The muscle alterations caused by one local boost of DUX4 expression constitute an easy read-out through a semi-automated histological quantification of the damaged area by color-thresholding **[44]**. Moreover, targeting the TA in this local FSHD model is pertinent as it is one of the most affected leg muscle in patients [70]. *Hif1α* mRNA level was increased in both the *pCIneo-DUX4* and *pCIneo* IMEP mice 6h post injection. The increase in the control plasmid group is likely linked to a muscle regeneration induced by the IMEP procedure. Indeed, an activation of Hif1α signaling was observed in injured TA muscle, increasing from day 1 to day 7 after a cardiotoxin injection [71]. One day post injection the increased *Hif1α* expression was only maintained in the *pCIneo-DUX4* group, meaning that this increase was DUX4-related.

In summary our data showed that DUX4 decreased *Hif1α mRNA* level in murine myoblast but increased it in mature myofibers in mice. Importantly, this induction was an early and transient event following DUX4 expression. Surprisingly, no modification could be detected in expression of Hif1α target genes *Pdk1* and *Vegf* in any experimental group and at any time points. Hif1α independent factors might prevent its transcriptional effect. We cannot exclude that this could result from limitations of the IMEP model (e.g. variability among animals). However, given that the model sensitivity was sufficient to highlight significant changes of *Hif1α* expression, these data suggested that both Hif1α-dependent and independent factors could influence *Pdk1* and *Vegf* expression levels. One hypothesis concerning these interfering factors is an activation of the muscle regeneration process [72]. Interestingly, Vegf was previously shown to play an important role in stimulating skeletal myofiber regeneration *in vivo*. Concerning *Pdk1*, other transcription factors are known to regulate *Pdk1* expression such as C-Myc or the Wnt pathway [73–76].

Targeted Hif1α knock down in mice exacerbates DUX4-induced muscle damages.

We wanted to specifically evaluate involvement of Hif1α in the development of DUX4 induced muscle lesions in our IMEP mouse model. We thus performed a loss of function study with siRNAs against *Hif1α mRNA* that we electroporated together with the *pCIneo-DUX4* transgene. The amount of *siRNA* we used caused about 2-fold *Hif1α* mRNA reduction. Surprisingly, a significant increase of muscle lesion area was observed upon *Hif1α* knock down but not with the control *siRNA*. The extension of muscle lesion we observed with specific *Hif1α* knock down could be explained by (**I**) a synergistic and negative effect of DUX4 and *siHIFs* on the myofibers itself or (**II**) a loss of the critical role of HIF1α in muscle regeneration, a process which mainly involves satellite cells but also fibro/adipogenic progenitors (FAPs) and immune cells. Concerning available evidences linking HIF1α and the regeneration process, it was shown that *Hif1α* silencing in C2C12 muscle cells or its chemical inhibition by echinomycin, significantly altered the differentiation process as shown by the decrease of *Myogenin* and *Myhc* expression **[50]**. In muscles of myeloid *Hif1α* KO mice, myoblast proliferation, regenerating fiber growth and macrophage invasion were delayed after trauma [77]. In IMEP model, *Hif1α* knock down could occur in myofibers but also in satellite cells where HIF1α is critical for their self-renewal

 doi:10.20944/preprints202211.0532.v2

and regeneration potency. Indeed, knock-out of HIF1α and HIF2α in satellite cells impedes muscle regeneration and decreases satellite cell number during this process [78].

The exacerbation of muscle lesion observed here upon HIF1α knockdown is contrasting with the results by Lek et al **[33]** obtained with FDA approved HIF signaling inhibitors. In these studies, FSHD-like zebrafish models (i.e. either single cell embryos injected with DUX4 *mRNA* or transgenic fish eggs with inducible DUX4 expression) were used and an improvement of muscle structure and function were observed. However, most of the drugs used were indirect inhibitors of HIF1α and had multiple effects. An indirect activity on protein turnover and therefore on DUX4 protein abundance could be a significant interfering factor. The reduction of DUX4 target gene expression observed in patient myotubes treated with Herbimycin (an inhibitor of PI3K/Akt/mTOR pathway), Rapamycin (an mTOR inhibitor), and Wortmannin and LY294002 (PI3K inhibitors) could reflect this interference. As well, only short-term effects were investigated. For a chronic treatment of muscle disorders, the negative effect of indirect inhibitors of HIF1α on protein synthesis should be avoided given the risk to exacerbate muscle atrophy. In addition, as we mentioned in **[41]**, drugs developed to interfere with HIF1α expression or activity were developed in order to induce targeted cancer cell death. This highlights the importance of the context of use when considering the action on HIF1α pathway. When zebrafish models were developed in an embryonic context, our results were obtained on mature fibers. Both DUX4 and HIF1 α are known to have specific activities during these two different conditions. This could explain the discrepancies observed in the results obtained. Because of its critical role in many skeletal muscle mechanisms, HIF1α remains challenging to target.

In conclusion, our study has set the basis for further investigations on the role of HIF1α in relationship with DUX4 in FSHD. However, we found that this link differed according to the muscle cell differentiation stage. Our results also suggested that this axis was conserved between human and mouse. Finally, we found that HIF1α silencing in an FSHD mouse model unexpectedly exacerbated the DUX4 mediated muscle damages. This indicated that the DUX4-HIF1α axis was not as simple as expected and that targeting HIF1α might be challenging in the context of FSHD therapeutic approaches. Finally, given (**I**) the regeneration defects in FSHD [79,80], (**II**) the role of HIF1α in this process **[41]**, (**III**) the impact of DUX4 expression on the HIF1α pathway depending on the differentiation state, further investigations, especially in satellite cells, appear critical for a better understanding of FSHD-associated muscle regeneration disturbances. Moreover, regarding the pivotal role of HIF1α in muscle metabolism, it will be important to clarify whether metabolic disturbances could contribute to the development of muscle dysfunction in FSHD. Such studies would provide more in-depth mechanistic insights into the FSHD pathogenic network and could suggest additional therapeutic targets.

4. Materials and Methods

4.1. Cell culture

Immortalized human myoblast cell lines (LHCN-iDUX4) were kindly provided by Prof. M.Kyba (Lillehei Heart Institute, University of Minnesota, Minneapolis). Cells were cultured in proliferation medium DMEM F12 (BioWest) supplemented with 20% FBS (Biowest), and 1% Penicillin/Streptomycin (P/S, Thermofisher) at 37 °C in a 5% CO_2 and atmospheric O_2 levels. For myogenic differentiation, cells were cultured on matrigel coated dishes (Corning) in proliferation medium until 100% confluence. Cells were then washed once with PBS and differentiated for two days for myocytes and four days for myotubes using differentiating medium (DMEM/F12 (Corning Cellgro), supplemented with human insulin 10 µg/ml (Sigma), bovine apo-transferrin 100 µg/ml (Sigma) and 1% Penicillin/Streptomycin (P/S, Thermofisher).

 doi:10.20944/preprints202211.0532.v2

Immortalized mouse myoblast cell lines (iC2C12-DUX4) were kindly provided by Prof. M. Kyba. They were cultured in proliferation medium DMEM high glucose (BioWest) supplemented with 10% FBS (Biowest), and 1% Penicillin/Streptomycin (P/S, Thermofisher) at 37 °C in a 5% CO_2 atmosphere.

4.2. Viability test

For the Vybrant® MTT Cell Proliferation Assay Kit (ThermoFisher), LHCN-iDUX4 et LHCN cells were seeded in a 96 well-plate and induced for 24h with doxycycline. Cells were then incubated for 2h with MTT 1.2 mM reagent diluted in proliferation medium at 37°C. After that step, medium was replaced by DMSO to solubilize the formazan product and the plate was incubated for 10 min at 37°C under agitation. The absorbance was then measured by a spectrophotometer (VERSA max-SoftMax Pro) at 540 nm.

For Cell Counting Kit-8 (Sigma), LHCN-iDUX4 and LHCN myoblasts were seeded in 96 well-plate and induced for 24h with doxycycline. Cells were then incubated for 1h with CCK-8 solution diluted in proliferation medium at 37°C. Absorbance was then measured by a spectrophotometer (VERSA max-SoftMax Pro) at 450 nm.

4.3. Myoblast transfection

10^5C2C12 cells were seeded in 6-well plates and transfected 24 hours later in Opti-MEM (Invitrogen, CA, USA) with 5µl of Lipofectamin 2000 (Invitrogen) and 1600 ng of DNA vector according to the manufacturer's instructions.

4.4. Immunofluorescence

Cells previously seeded in 6-well plate on glass slide, were fixed with 4% paraformaldehyde/PBS for 10 min, permeabilized with 0.5% TritonX-100/PBS for 10 min, then incubated with blocking solution (5% normal goat serum (Biowest), TritonX-100/PBS) for 1h at room temperature. Cells were then incubated with primary antibodies (anti-DUX4 9A12 MABD116; 1:100, Merck (**[53]**); HIF1α ab179483, 1:500, Abcam) at 4 °C overnight. They were subsequently rinsed in PBS and incubated with secondary antibodies Alexa 555 Goat anti-rabbit IgG (1:500, Biotium) and Alexa 488 Goat anti-mouse IgG (1:500, Biotium) at room temperature for 1 h. Immunolabelled cells were rinsed in PBS and mounted with EverBrite Mounting Medium with DAPI (Biotium) for nuclear staining. Pictures were taken with a Nikon Eclipse 80i microscope and merged using NIS-Elements software.

4.5. qPCR

RNA was extracted using Trizol reagent (Invitrogen) according to the manufacturer's directions. Total RNA was then treated with DNAse I (amplification grade, ThermoFisher). cDNAs were synthetized using Maxima First Strand cDNA Synthesis kit (ThermoFisher). All qPCRs were performed in triplicates using SYBR Green FastStart Essential DNA Green Master (Roche) and corresponding primers (Eurogentec) (See Supplementary materials). Cycling conditions were as follows: initial denaturation step at 95 °C for 10 min, followed by 40 cycles of 15 s at 95 °C and 60 s at primer Tm. qPCR results were analyzed with LightCycler 96 software (Roche). Quantifications were performed using the $2^{-\Delta\Delta Ct}$ method.

4.6. Western Blot

Cells were lysed using RIPA buffer. Proteins were separated on 12% SDS-PAGE gels for 3h at 100V and transferred to nitrocellulose membrane for 1h45 at 260 mA. Membrane blocking was performed using 5% non fat dry milk diluted in TBST-T. Primary (PDK1, ab110025, Abcam) and secondary HRP conjugated antibody (NA931, ECL) were diluted in 5% skim milk in TBST and incubated overnight at 4 °C and 1 hour at room temperature

 doi:10.20944/preprints202211.0532.v2

respectively. HRP signal was visualized using Supersignal West Femto max. sensitivity kit (Thermo Scientific) and the Fusion FX7 spectra (Vilber)

4.7. Ethics statement

All animal experiments met the Belgian national standard requirements regarding animal care and were conducted in accordance with the Ethics and Welfare Committee of the University of Mons (reference number LE018/02)

4.8. IMEP mouse model

Female C57BL/6 mice, aged between 8 and 12 weeks, were purchase from Charles River laboratories (France). Mice were housed in a conventional animal colony and maintained at 35–40% relative humidity with a constant room temperature (21 °C) and natural day/night light cycle (12–12 h). Food and water were provided ad libitum and animals were subjected to an adaptation period of 7 days before experiments. IMEP model was generated as previously described **[44]**. Briefly, tibialis anterior (TA) muscles were injected with 40 μg of hyaluronidase. Each TA was then injected with either naked plasmid DNA alone or complemented with siRNA targeting HIF1α RNA (siHIF; Qiagen, #1027416) or control (siCTL; Qiagen, #1027280) and electroporated using an EMKA stimulator. Mice were checked daily and then sacrificed by an intraperitoneal injection of Nembutal (Kela).

4.9. Tissue preparation and histology

At the indicated euthanasia time points, right and left TAs were removed, embedded in OCT compound (VWR) and frozen in liquid nitrogen-cooled isopentane. 8 μm thick cryostat sections from proximal and medial of TA were cut using a Leica cryotome and sections were stained with Hematoxylin–Eosin–Heidenhain blue (HEB) to evaluate the percentage of muscle lesions. HEB staining consists in a basic Hematoxylin–Eosin coloration followed by a 45-s incubation in Heidenhain's Blue staining (mix of orange G and Aniline Blue, Sigma-Aldrich, USA), allowing an intense blue labeling of fibrotic fibers and collagenous tissues. Slides were then scanned using the NanoZoomer-SQ Digital slide scanner (Hamamatsu Photonics). Images were processed as described in **[44]**.

5. Statistical analysis

Normality tests (Shapiro-Wilk) were performed on each data sets to assess the data distribution and thus appropriate statistic tests could be chosen. Differences were considered statistically significant at a p-value < 0.05. All data were represented as mean +/- SEM or boxplot (5 and 95th percentile) for parametric or non-parametric statistical tests, respectively. Statistical analyses were done using GraphPad Prism software, version 8.02 and SigmaPlot software, version 14.

Acknowledgments: We would like to thank Pr. M. Kyba for providing the human and mouse myoblast lines.

Author Contributions: Conceptualization, Thuy-Hang Nguyen, Anne-Emilie Declèves, Philipp Heher, Alexandra Belayew, Christopher R. S. Banerji, Peter S. Zammit and Alexandra Tassin; Data curation, Thuy-Hang Nguyen, Sihame Bouhmidi, Lise Paprzycki, Alexandre Legrand, Anne-Emilie Declèves and Alexandra Tassin; Funding acquisition, Thuy-Hang Nguyen and Alexandra Tassin; Investigation, Thuy-Hang Nguyen, Sihame Bouhmidi and Lise Paprzycki; Supervision, Alexandre Legrand and Alexandra Tassin; Writing – original draft, Thuy-Hang Nguyen, Alexandre Legrand, Alexandra Belayew and Alexandra Tassin; Writing – review & editing, Thuy-Hang Nguyen, Alexandre Legrand, Anne-Emilie Declèves, Philipp Heher, Alexandra Belayew, Christopher R. S. Banerji, Peter S. Zammit and Alexandra Tassin.

Fundings: T.-H.N. holds a FRIA doctoral fellowship (FC 29703) from the National Fund for Scientific Research (F.R.S – FNRS), Belgium. T.-H.N. acknowledges funding from Amis FSH, ABMM and AFM Telethon. This work was supported by the Fonds de la Recherche Scientifique - FNRS under Grant(s) n° Equipment UN07220F. PH was mainly funded by the Medical Research Council (MR/P023215/1) and then by an Erwin Schroedinger post-doctoral fellowship awarded by the Austrian Science Fund (FWF, J4435-B), supported by Friends of FSH Research (Project 936270) and the FSHD Society (FSHD-Fall2020-3308289076).

Conflicts of Interest: The authors declare no conflict of interest.

References

1. Lemmers, R.J.L.F.; van der Vliet, P.J.; Klooster, R.; Sacconi, S.; Camaño, P.; Dauwerse, J.G.; Snider, L.; Straasheijm, K.R.; van Ommen, G.J.; Padberg, G.W.; et al. A Unifying Genetic Model for Facioscapulohumeral Muscular Dystrophy. *Science* **2010**, *329*, 1650–1653, doi:10.1126/science.1189044.
2. Gabriëls, J.; Beckers, M.C.; Ding, H.; De Vriese, A.; Plaisance, S.; van der Maarel, S.M.; Padberg, G.W.; Frants, R.R.; Hewitt, J.E.; Collen, D.; et al. Nucleotide Sequence of the Partially Deleted D4Z4 Locus in a Patient with FSHD Identifies a Putative Gene within Each 3.3 Kb Element. *Gene* **1999**, *236*, 25–32.
3. Dixit, M.; Ansseau, E.; Tassin, A.; Winokur, S.; Shi, R.; Qian, H.; Sauvage, S.; Mattéotti, C.; van Acker, A.M.; Leo, O.; et al. DUX4, a Candidate Gene of Facioscapulohumeral Muscular Dystrophy, Encodes a Transcriptional Activator of PITX1. *Proc. Natl. Acad. Sci. U. S. A.* **2007**, *104*, 18157–18162, doi:10.1073/pnas.0708659104.
4. Banerji, C.R.S.; Zammit, P.S. Pathomechanisms and Biomarkers in Facioscapulohumeral Muscular Dystrophy: Roles of DUX4 and PAX7. *EMBO Mol. Med.* **2021**, *n/a*, e13695, doi:10.15252/emmm.202013695.
5. Wang, L.H.; Tawil, R. Facioscapulohumeral Dystrophy. *Curr. Neurol. Neurosci. Rep.* **2016**, *16*, 66, doi:10.1007/s11910-016-0667-0.
6. Chen, T.-H.; Wu, Y.-Z.; Tseng, Y.-H. Early-Onset Infantile Facioscapulohumeral Muscular Dystrophy: A Timely Review. *Int. J. Mol. Sci.* **2020**, *21*, 7783, doi:10.3390/ijms21207783.
7. De Iaco, A.; Planet, E.; Coluccio, A.; Verp, S.; Duc, J.; Trono, D. DUX-Family Transcription Factors Regulate Zygotic Genome Activation in Placental Mammals. *Nat. Genet.* **2017**, *49*, 941–945, doi:10.1038/ng.3858.
8. Hendrickson, P.G.; Doráis, J.A.; Grow, E.J.; Whiddon, J.L.; Lim, J.-W.; Wike, C.L.; Weaver, B.D.; Pflueger, C.; Emery, B.R.; Wilcox, A.L.; et al. Conserved Roles of Mouse DUX and Human DUX4 in Activating Cleavage-Stage Genes and MERVL/HERVL Retrotransposons. *Nat. Genet.* **2017**, *49*, 925–934, doi:10.1038/ng.3844.
9. Bosnakovski, D.; Gearhart, M.D.; Ho Choi, S.; Kyba, M. Dux Facilitates Post-Implantation Development, but Is Not Essential for Zygotic Genome Activation†. *Biol. Reprod.* **2021**, *104*, 83–93, doi:10.1093/biolre/ioaa179.
10. Ryhove, L. de la K. de; Ansseau, E.; Geens, M.; Coppée, F.; Sermon, K.D.; Lagneaux, L.; Belayew, A. DUX4 Expression during Osteogenic Differentiation in Mesenchymal Stromal Cells (MSCs). *Cytotherapy* **2014**, *16*, S65, doi:10.1016/j.jcyt.2014.01.238.
11. Gannon, O.M.; Merida de Long, L.; Saunders, N.A. DUX4 Is Derepressed in Late-Differentiating Keratinocytes in Conjunction with Loss of H3K9me3 Epigenetic Repression. *J. Invest. Dermatol.* **2016**, *136*, 1299–1302, doi:10.1016/j.jid.2016.01.027.
12. Wijmenga, C.; Hewitt, J.E.; Sandkuijl, L.A.; Clark, L.N.; Wright, T.J.; Dauwerse, H.G.; Gruter, A.M.; Hofker, M.H.; Moerer, P.; Williamson, R. Chromosome 4q DNA Rearrangements Associated with Facioscapulohumeral Muscular Dystrophy. *Nat. Genet.* **1992**, *2*, 26–30, doi:10.1038/ng0992-26.

13. van Deutekom, J.C.; Wijmenga, C.; van Tienhoven, E.A.; Gruter, A.M.; Hewitt, J.E.; Padberg, G.W.; van Ommen, G.J.; Hofker, M.H.; Frants, R.R. FSHD Associated DNA Rearrangements Are Due to Deletions of Integral Copies of a 3.2 Kb Tandemly Repeated Unit. *Hum. Mol. Genet.* **1993**, *2*, 2037–2042.
14. Sacconi, S.; Briand-Suleau, A.; Gros, M.; Baudoin, C.; Lemmers, R.J.L.F.; Rondeau, S.; Lagha, N.; Nigumann, P.; Cambieri, C.; Puma, A.; et al. FSHD1 and FSHD2 Form a Disease Continuum. *Neurology* **2019**, *92*, e2273–e2285, doi:10.1212/WNL.0000000000007456.
15. Sacconi, S.; Lemmers, R.J.L.F.; Balog, J.; van der Vliet, P.J.; Lahaut, P.; van Nieuwenhuizen, M.P.; Straasheijm, K.R.; Debipersad, R.D.; Vos-Versteeg, M.; Salviati, L.; et al. The FSHD2 Gene SMCHD1 Is a Modifier of Disease Severity in Families Affected by FSHD1. *Am. J. Hum. Genet.* **2013**, *93*, 744–751, doi:10.1016/j.ajhg.2013.08.004.
16. Lemmers, R.J.L.F.; van den Boogaard, M.L.; van der Vliet, P.J.; Donlin-Smith, C.M.; Nations, S.P.; Ruivenkamp, C.A.L.; Heard, P.; Bakker, B.; Tapscott, S.; Cody, J.D.; et al. Hemizygosity for SMCHD1 in Facioscapulohumeral Muscular Dystrophy Type 2: Consequences for 18p Deletion Syndrome. *Hum. Mutat.* **2015**, *36*, 679–683, doi:10.1002/humu.22792.
17. Geng, L.N.; Yao, Z.; Snider, L.; Fong, A.P.; Cech, J.N.; Young, J.M.; van der Maarel, S.M.; Ruzzo, W.L.; Gentleman, R.C.; Tawil, R.; et al. DUX4 Activates Germline Genes, Retroelements and Immune-Mediators: Implications for Facioscapulohumeral Dystrophy. *Dev. Cell* **2012**, *22*, 38–51, doi:10.1016/j.devcel.2011.11.013.
18. Snider, L.; Geng, L.N.; Lemmers, R.J.L.F.; Kyba, M.; Ware, C.B.; Nelson, A.M.; Tawil, R.; Filippova, G.N.; van der Maarel, S.M.; Tapscott, S.J.; et al. Facioscapulohumeral Dystrophy: Incomplete Suppression of a Retrotransposed Gene. *PLoS Genet.* **2010**, *6*, doi:10.1371/journal.pgen.1001181.
19. Vanderplanck, C.; Ansseau, E.; Charron, S.; Stricwant, N.; Tassin, A.; Laoudj-Chenivesse, D.; Wilton, S.D.; Coppée, F.; Belayew, A. The FSHD Atrophic Myotube Phenotype Is Caused by DUX4 Expression. *PLOS ONE* **2011**, *6*, e26820, doi:10.1371/journal.pone.0026820.
20. Lim, K.R.Q.; Nguyen, Q.; Yokota, T. DUX4 Signalling in the Pathogenesis of Facioscapulohumeral Muscular Dystrophy. *Int. J. Mol. Sci.* **2020**, *21*, doi:10.3390/ijms21030729.
21. Banerji, C.R.S.; Panamarova, M.; Hebaishi, H.; White, R.B.; Relaix, F.; Severini, S.; Zammit, P.S. PAX7 Target Genes Are Globally Repressed in Facioscapulohumeral Muscular Dystrophy Skeletal Muscle. *Nat. Commun.* **2017**, *8*, 2152, doi:10.1038/s41467-017-01200-4.
22. Banerji, C.R.S. PAX7 Target Gene Repression Associates with FSHD Progression and Pathology over 1 Year. *Hum. Mol. Genet.* **2020**, *29*, 2124–2133, doi:10.1093/hmg/ddaa079.
23. Bosnakovski, D.; Xu, Z.; Gang, E.J.; Galindo, C.L.; Liu, M.; Simsek, T.; Garner, H.R.; Agha-Mohammadi, S.; Tassin, A.; Coppée, F.; et al. An Isogenetic Myoblast Expression Screen Identifies DUX4-Mediated FSHD-Associated Molecular Pathologies. *EMBO J.* **2008**, *27*, 2766–2779, doi:10.1038/emboj.2008.201.
24. Bosnakovski, D.; Gearhart, M.D.; Toso, E.A.; Ener, E.T.; Choi, S.H.; Kyba, M. Low Level DUX4 Expression Disrupts Myogenesis through Deregulation of Myogenic Gene Expression. *Sci. Rep.* **2018**, *8*, 16957, doi:10.1038/s41598-018-35150-8.
25. Heher, P.; Ganassi, M.; Weidinger, A.; Engquist, E.N.; Pruller, J.; Nguyen, T.H.; Tassin, A.; Declèves, A.-E.; Mamchaoui, K.; Banerji, C.R.S.; et al. Interplay between Mitochondrial Reactive Oxygen Species, Oxidative Stress and Hypoxic Adaptation in Facioscapulohumeral Muscular Dystrophy: Metabolic Stress as Potential Therapeutic Target. *Redox Biol.* **2022**, *51*, 102251, doi:10.1016/j.redox.2022.102251.

26. Celegato, B.; Capitanio, D.; Pescatori, M.; Romualdi, C.; Pacchioni, B.; Cagnin, S.; Viganò, A.; Colantoni, L.; Begum, S.; Ricci, E.; et al. Parallel Protein and Transcript Profiles of FSHD Patient Muscles Correlate to the D4Z4 Arrangement and Reveal a Common Impairment of Slow to Fast Fibre Differentiation and a General Deregulation of MyoD-Dependent Genes. *PROTEOMICS* **2006**, *6*, 5303–5321, doi:10.1002/pmic.200600056.
27. Jagannathan, S.; Ogata, Y.; Gafken, P.R.; Tapscott, S.J.; Bradley, R.K. Quantitative Proteomics Reveals Key Roles for Post-Transcriptional Gene Regulation in the Molecular Pathology of Facioscapulohumeral Muscular Dystrophy. *eLife* **2019**, *8*, e41740, doi:10.7554/eLife.41740.
28. Rickard, A.M.; Petek, L.M.; Miller, D.G. Endogenous DUX4 Expression in FSHD Myotubes Is Sufficient to Cause Cell Death and Disrupts RNA Splicing and Cell Migration Pathways. *Hum. Mol. Genet.* **2015**, *24*, 5901–5914, doi:10.1093/hmg/ddv315.
29. Ansseau, E.; Eidahl, J.O.; Lancelot, C.; Tassin, A.; Matteotti, C.; Yip, C.; Liu, J.; Leroy, B.; Hubeau, C.; Gerbaux, C.; et al. Homologous Transcription Factors DUX4 and DUX4c Associate with Cytoplasmic Proteins during Muscle Differentiation. *PloS One* **2016**, *11*, e0146893, doi:10.1371/journal.pone.0146893.
30. DeSimone, A.M.; Leszyk, J.; Wagner, K.; Emerson, C.P. Identification of the Hyaluronic Acid Pathway as a Therapeutic Target for Facioscapulohumeral Muscular Dystrophy. *Sci. Adv.* **2019**, *5*, eaaw7099, doi:10.1126/sciadv.aaw7099.
31. Banerji, C.R.S.; Knopp, P.; Moyle, L.A.; Severini, S.; Orrell, R.W.; Teschendorff, A.E.; Zammit, P.S. β-Catenin Is Central to DUX4-Driven Network Rewiring in Facioscapulohumeral Muscular Dystrophy. *J. R. Soc. Interface* **2015**, *12*, 20140797.
32. Tsumagari, K.; Chang, S.-C.; Lacey, M.; Baribault, C.; Chittur, S.V.; Sowden, J.; Tawil, R.; Crawford, G.E.; Ehrlich, M. Gene Expression during Normal and FSHD Myogenesis. *BMC Med. Genomics* **2011**, *4*, 67, doi:10.1186/1755-8794-4-67.
33. Lek, A.; Zhang, Y.; Woodman, K.G.; Huang, S.; DeSimone, A.M.; Cohen, J.; Ho, V.; Conner, J.; Mead, L.; Kodani, A.; et al. Applying Genome-Wide CRISPR-Cas9 Screens for Therapeutic Discovery in Facioscapulohumeral Muscular Dystrophy. *Sci. Transl. Med.* **2020**, *12*, doi:10.1126/scitranslmed.aay0271.
34. Koh, M.Y.; Spivak-Kroizman, T.R.; Powis, G. HIF-1 Regulation: Not so Easy Come, Easy Go. *Trends Biochem. Sci.* **2008**, *33*, 526–534, doi:10.1016/j.tibs.2008.08.002.
35. Macklin, P.S.; Yamamoto, A.; Browning, L.; Hofer, M.; Adam, J.; Pugh, C.W. Recent Advances in the Biology of Tumour Hypoxia with Relevance to Diagnostic Practice and Tissue-Based Research. *J. Pathol.* **2020**, *250*, 593–611, doi:10.1002/path.5402.
36. Muz, B.; de la Puente, P.; Azab, F.; Azab, A.K. The Role of Hypoxia in Cancer Progression, Angiogenesis, Metastasis, and Resistance to Therapy. *Hypoxia* **2015**, *3*, 83–92, doi:10.2147/HP.S93413.
37. De Iaco, A.; Verp, S.; Offner, S.; Grun, D.; Trono, D. DUX Is a Non-Essential Synchronizer of Zygotic Genome Activation. *Dev. Camb. Engl.* **2020**, *147*, doi:10.1242/dev.177725.
38. Semenza, G.L. HIF-1, O(2), and the 3 PHDs: How Animal Cells Signal Hypoxia to the Nucleus. *Cell* **2001**, *107*, 1–3, doi:10.1016/s0092-8674(01)00518-9.
39. De Palma, S.; Ripamonti, M.; Viganò, A.; Moriggi, M.; Capitanio, D.; Samaja, M.; Milano, G.; Cerretelli, P.; Wait, R.; Gelfi, C. Metabolic Modulation Induced by Chronic Hypoxia in Rats Using a Comparative Proteomic Analysis of Skeletal Muscle Tissue. *J. Proteome Res.* **2007**, *6*, 1974–1984, doi:10.1021/pr060614o.
40. Zhang, S.; Hulver, M.W.; McMillan, R.P.; Cline, M.A.; Gilbert, E.R. The Pivotal Role of Pyruvate Dehydrogenase Kinases in Metabolic Flexibility. *Nutr. Metab.* **2014**, *11*, 10, doi:10.1186/1743-7075-11-10.

41. Nguyen, T.-H.; Conotte, S.; Belayew, A.; Declèves, A.-E.; Legrand, A.; Tassin, A. Hypoxia and Hypoxia-Inducible Factor Signaling in Muscular Dystrophies: Cause and Consequences. *Int. J. Mol. Sci.* **2021**, *22*, 7220, doi:10.3390/ijms22137220.
42. Banerji, C.R.S.; Panamarova, M.; Pruller, J.; Figeac, N.; Hebaishi, H.; Fidanis, E.; Saxena, A.; Contet, J.; Sacconi, S.; Severini, S.; et al. Dynamic Transcriptomic Analysis Reveals Suppression of PGC1α/ERRα Drives Perturbed Myogenesis in Facioscapulohumeral Muscular Dystrophy. *Hum. Mol. Genet.* **2019**, *28*, 1244–1259, doi:10.1093/hmg/ddy405.
43. Barro, M.; Carnac, G.; Flavier, S.; Mercier, J.; Vassetzky, Y.; Laoudj-Chenivesse, D. Myoblasts from Affected and Non-Affected FSHD Muscles Exhibit Morphological Differentiation Defects. *J. Cell. Mol. Med.* **2010**, *14*, 275–289, doi:10.1111/j.1582-4934.2008.00368.x.
44. Derenne, A.; Tassin, A.; Nguyen, T.H.; De Roeck, E.; Jenart, V.; Ansseau, E.; Belayew, A.; Coppée, F.; Declèves, A.-E.; Legrand, A. Induction of a Local Muscular Dystrophy Using Electroporation in Vivo: An Easy Tool for Screening Therapeutics. *Sci. Rep.* **2020**, *10*, 11301, doi:10.1038/s41598-020-68135-7.
45. Zhu, C.-H.; Mouly, V.; Cooper, R.N.; Mamchaoui, K.; Bigot, A.; Shay, J.W.; Di Santo, J.P.; Butler-Browne, G.S.; Wright, W.E. Cellular Senescence in Human Myoblasts Is Overcome by Human Telomerase Reverse Transcriptase and Cyclin-Dependent Kinase 4: Consequences in Aging Muscle and Therapeutic Strategies for Muscular Dystrophies. *Aging Cell* **2007**, *6*, 515–523, doi:10.1111/j.1474-9726.2007.00306.x.
46. Choi, S.H.; Gearhart, M.D.; Cui, Z.; Bosnakovski, D.; Kim, M.; Schennum, N.; Kyba, M. DUX4 Recruits P300/CBP through Its C-Terminus and Induces Global H3K27 Acetylation Changes. *Nucleic Acids Res.* **2016**, *44*, 5161–5173, doi:10.1093/nar/gkw141.
47. Pandey, S.N.; Khawaja, H.; Chen, Y.-W. Culture Conditions Affect Expression of DUX4 in FSHD Myoblasts. *Molecules* **2015**, *20*, 8304–8315, doi:10.3390/molecules20058304.
48. Pirkmajer, S.; Filipovic, D.; Mars, T.; Mis, K.; Grubic, Z. HIF-1α Response to Hypoxia Is Functionally Separated from the Glucocorticoid Stress Response in the in Vitro Regenerating Human Skeletal Muscle. *Am. J. Physiol.-Regul. Integr. Comp. Physiol.* **2010**, *299*, R1693–R1700, doi:10.1152/ajpregu.00133.2010.
49. Dehne, N.; Kerkweg, U.; Otto, T.; Fandrey, J. The HIF-1 Response to Simulated Ischemia in Mouse Skeletal Muscle Cells Neither Enhances Glycolysis nor Prevents Myotube Cell Death. *Am. J. Physiol.-Regul. Integr. Comp. Physiol.* **2007**, *293*, R1693–R1701, doi:10.1152/ajpregu.00892.2006.
50. Cirillo, F.; Resmini, G.; Ghiroldi, A.; Piccoli, M.; Bergante, S.; Tettamanti, G.; Anastasia, L. Activation of the Hypoxia-Inducible Factor 1a Promotes Myogenesis through the Noncanonical Wnt Pathway, Leading to Hypertrophic Myotubes. *FASEB J.* **2017**, *31*, 2146–2156, doi:https://doi.org/10.1096/fj.201600878R.
51. Chen, R.; Jiang, T.; She, Y.; Xu, J.; Li, C.; Zhou, S.; Shen, H.; Shi, H.; Liu, S. Effects of Cobalt Chloride, a Hypoxia-Mimetic Agent, on Autophagy and Atrophy in Skeletal C2C12 Myotubes. *BioMed Res. Int.* **2017**, *2017*, doi:10.1155/2017/7097580.
52. Winokur, S.T.; Barrett, K.; Martin, J.H.; Forrester, J.R.; Simon, M.; Tawil, R.; Chung, S.-A.; Masny, P.S.; Figlewicz, D.A. Facioscapulohumeral Muscular Dystrophy (FSHD) Myoblasts Demonstrate Increased Susceptibility to Oxidative Stress. *Neuromuscul. Disord. NMD* **2003**, *13*, 322–333, doi:10.1016/s0960-8966(02)00284-5.
53. Tassin, A.; Laoudj-Chenivesse, D.; Vanderplanck, C.; Barro, M.; Charron, S.; Ansseau, E.; Chen, Y.-W.; Mercier, J.; Coppée, F.; Belayew, A. DUX4 Expression in FSHD Muscle Cells: How Could Such a Rare Protein Cause a Myopathy? *J. Cell. Mol. Med.* **2013**, *17*, 76–89, doi:10.1111/j.1582-4934.2012.01647.x.
54. Hagen, T. Oxygen versus Reactive Oxygen in the Regulation of HIF-1α: The Balance Tips. *Biochem. Res. Int.* **2012**, *2012*, 436981, doi:10.1155/2012/436981.

55. Turki, A.; Hayot, M.; Carnac, G.; Pillard, F.; Passerieux, E.; Bommart, S.; Raynaud de Mauverger, E.; Hugon, G.; Pincemail, J.; Pietri, S.; et al. Functional Muscle Impairment in Facioscapulohumeral Muscular Dystrophy Is Correlated with Oxidative Stress and Mitochondrial Dysfunction. *Free Radic. Biol. Med.* **2012**, *53*, 1068–1079, doi:10.1016/j.freeradbiomed.2012.06.041.
56. Passerieux, E.; Hayot, M.; Jaussent, A.; Carnac, G.; Gouzi, F.; Pillard, F.; Picot, M.-C.; Böcker, K.; Hugon, G.; Pincemail, J.; et al. Effects of Vitamin C, Vitamin E, Zinc Gluconate, and Selenomethionine Supplementation on Muscle Function and Oxidative Stress Biomarkers in Patients with Facioscapulohumeral Dystrophy: A Double-Blind Randomized Controlled Clinical Trial. *Free Radic. Biol. Med.* **2015**, *81*, 158–169, doi:10.1016/j.freeradbiomed.2014.09.014.
57. Wilson, V.D.; Thomas, C.; Passerieux, E.; Hugon, G.; Pillard, F.; Andrade, A.G.; Bommart, S.; Picot, M.-C.; Pincemail, J.; Mercier, J.; et al. Impaired Oxygen Demand during Exercise Is Related to Oxidative Stress and Muscle Function in Facioscapulohumeral Muscular Dystrophy. *JCSM Rapid Commun.* **2018**, *1*, 1–13, doi:https://doi.org/10.1002/j.2617-1619.2018.tb00002.x.
58. Sasaki-Honda, M.; Jonouchi, T.; Arai, M.; Hotta, A.; Mitsuhashi, S.; Nishino, I.; Matsuda, R.; Sakurai, H. A Patient-Derived IPSC Model Revealed Oxidative Stress Increases Facioscapulohumeral Muscular Dystrophy-Causative DUX4. *Hum. Mol. Genet.* **2018**, *27*, 4024–4035, doi:10.1093/hmg/ddy293.
59. Karpukhina, A.; Galkin, I.; Ma, Y.; Dib, C.; Zinovkin, R.; Pletjushkina, O.; Chernyak, B.; Popova, E.; Vassetzky, Y. Analysis of Genes Regulated by DUX4 via Oxidative Stress Reveals Potential Therapeutic Targets for Treatment of Facioscapulohumeral Dystrophy. *Redox Biol.* **2021**, *43*, 102008, doi:10.1016/j.redox.2021.102008.
60. Mosca, N.; Petrillo, S.; Bortolani, S.; Monforte, M.; Ricci, E.; Piemonte, F.; Tasca, G. Redox Homeostasis in Muscular Dystrophies. *Cells* **2021**, *10*, 1364, doi:10.3390/cells10061364.
61. Fortini, P.; Ferretti, C.; Iorio, E.; Cagnin, M.; Garribba, L.; Pietraforte, D.; Falchi, M.; Pascucci, B.; Baccarini, S.; Morani, F.; et al. The Fine Tuning of Metabolism, Autophagy and Differentiation during in Vitro Myogenesis. *Cell Death Dis.* **2016**, *7*, e2168–e2168, doi:10.1038/cddis.2016.50.
62. Knopp, P.; Krom, Y.D.; Banerji, C.R.S.; Panamarova, M.; Moyle, L.A.; den Hamer, B.; van der Maarel, S.M.; Zammit, P.S. DUX4 Induces a Transcriptome More Characteristic of a Less-Differentiated Cell State and Inhibits Myogenesis. *J. Cell Sci.* **2016**, *129*, 3816–3831, doi:10.1242/jcs.180372.
63. Cerychova, R.; Pavlinkova, G. HIF-1, Metabolism, and Diabetes in the Embryonic and Adult Heart. *Front. Endocrinol.* **2018**, *9*, 460, doi:10.3389/fendo.2018.00460.
64. Wang, X.; Shen, X.; Yan, Y.; Li, H. Pyruvate Dehydrogenase Kinases (PDKs): An Overview toward Clinical Applications. *Biosci. Rep.* **2021**, *41*, BSR20204402, doi:10.1042/BSR20204402.
65. Pajares, M.; Jiménez-Moreno, N.; Dias, I.H.K.; Debelec, B.; Vucetic, M.; Fladmark, K.E.; Basaga, H.; Ribaric, S.; Milisav, I.; Cuadrado, A. Redox Control of Protein Degradation. *Redox Biol.* **2015**, *6*, 409–420, doi:10.1016/j.redox.2015.07.003.
66. Statland, J.M.; Odrzywolski, K.J.; Shah, B.; Henderson, D.; Fricke, A.F.; van der Maarel, S.M.; Tapscott, S.J.; Tawil, R. Immunohistochemical Characterization of FacioscapulohumeralMuscular Dystrophy Muscle Biopsies. *J. Neuromuscul. Dis.* **2015**, *2*, 291–299, doi:10.3233/JND-150077.
67. Shields, C.L.; Zahler, J.; Falk, N.; Furuta, M.; Eagle, R.C.; Espinosa, L.E.B.; Fischer, P.R.; Shields, J.A. Neovascular Glaucoma from Advanced Coats Disease as the Initial Manifestation of Facioscapulohumeral Dystrophy in a 2-Year-Old Child. *Arch. Ophthalmol. Chic. Ill 1960* **2007**, *125*, 840–842, doi:10.1001/archopht.125.6.840.
68. Goselink, R.J.M.; Schreur, V.; van Kernebeek, C.R.; Padberg, G.W.; van der Maarel, S.M.; van Engelen, B.G.M.; Erasmus, C.E.; Theelen, T. Ophthalmological Findings in Facioscapulohumeral Dystrophy. *Brain Commun.* **2019**, *1*, doi:10.1093/braincomms/fcz023.

69. Fitzsimons, R.B. Retinal Vascular Disease and the Pathogenesis of Facioscapulohumeral Muscular Dystrophy. A Signalling Message from Wnt? *Neuromuscul. Disord.* **2011**, *21*, 263–271, doi:10.1016/j.nmd.2011.02.002.
70. Olsen, D.B.; Gideon, P.; Jeppesen, T.D.; Vissing, J. Leg Muscle Involvement in Facioscapulohumeral Muscular Dystrophy Assessed by MRI. *J. Neurol.* **2006**, *253*, 1437–1441, doi:10.1007/s00415-006-0230-z.
71. Drouin, G.; Couture, V.; Lauzon, M.-A.; Balg, F.; Faucheux, N.; Grenier, G. Muscle Injury-Induced Hypoxia Alters the Proliferation and Differentiation Potentials of Muscle Resident Stromal Cells. *Skelet. Muscle* **2019**, *9*, 18, doi:10.1186/s13395-019-0202-5.
72. Arsic, N.; Zacchigna, S.; Zentilin, L.; Ramirez-Correa, G.; Pattarini, L.; Salvi, A.; Sinagra, G.; Giacca, M. Vascular Endothelial Growth Factor Stimulates Skeletal Muscle Regeneration in Vivo. *Mol. Ther.* **2004**, *10*, 844–854, doi:10.1016/j.ymthe.2004.08.007.
73. Li, Z.; Van Calcar, S.; Qu, C.; Cavenee, W.K.; Zhang, M.Q.; Ren, B. A Global Transcriptional Regulatory Role for C-Myc in Burkitt's Lymphoma Cells. *Proc. Natl. Acad. Sci. U. S. A.* **2003**, *100*, 8164–8169, doi:10.1073/pnas.1332764100.
74. Kim, J.; Gao, P.; Liu, Y.-C.; Semenza, G.L.; Dang, C.V. Hypoxia-Inducible Factor 1 and Dysregulated c-Myc Cooperatively Induce Vascular Endothelial Growth Factor and Metabolic Switches Hexokinase 2 and Pyruvate Dehydrogenase Kinase 1. *Mol. Cell. Biol.* **2007**, *27*, 7381–7393, doi:10.1128/MCB.00440-07.
75. Pate, K.T.; Stringari, C.; Sprowl-Tanio, S.; Wang, K.; TeSlaa, T.; Hoverter, N.P.; McQuade, M.M.; Garner, C.; Digman, M.A.; Teitell, M.A.; et al. Wnt Signaling Directs a Metabolic Program of Glycolysis and Angiogenesis in Colon Cancer. *EMBO J.* **2014**, *33*, 1454–1473, doi:10.15252/embj.201488598.
76. Lee, M.; Chen, G.T.; Puttock, E.; Wang, K.; Edwards, R.A.; Waterman, M.L.; Lowengrub, J. Mathematical Modeling Links Wnt Signaling to Emergent Patterns of Metabolism in Colon Cancer. *Mol. Syst. Biol.* **2017**, *13*, 912, doi:10.15252/msb.20167386.
77. Scheerer, N.; Dehne, N.; Stockmann, C.; Swoboda, S.; Baba, H.A.; Neugebauer, A.; Johnson, R.S.; Fandrey, J. Myeloid Hypoxia-Inducible Factor-1α Is Essential for Skeletal Muscle Regeneration in Mice. *J. Immunol. Baltim. Md 1950* **2013**, *191*, 407–414, doi:10.4049/jimmunol.1103779.
78. Yang, X.; Yang, S.; Wang, C.; Kuang, S. The Hypoxia-Inducible Factors HIF1α and HIF2α Are Dispensable for Embryonic Muscle Development but Essential for Postnatal Muscle Regeneration. *J. Biol. Chem.* **2017**, *292*, 5981–5991, doi:10.1074/jbc.M116.756312.
79. Di Pietro, L.; Giacalone, F.; Ragozzino, E.; Saccone, V.; Tiberio, F.; De Bardi, M.; Picozza, M.; Borsellino, G.; Lattanzi, W.; Guadagni, E.; et al. Non-Myogenic Mesenchymal Cells Contribute to Muscle Degeneration in Facioscapulohumeral Muscular Dystrophy Patients. *Cell Death Dis.* **2022**, *13*, 793, doi:10.1038/s41419-022-05233-6.
80. Ganassi, M.; Zammit, P.S. Involvement of Muscle Satellite Cell Dysfunction in Neuromuscular Disorders: Expanding the Portfolio of Satellite Cell-Opathies. *Eur. J. Transl. Myol.* **2022**, *32*, doi:10.4081/ejtm.2022.10064.